



Discovery of 4-alkoxy-2-aryl-6,7-dimethoxyquinolines as a new class of topoisomerase I inhibitors endowed with potent *in vitro* anticancer activity



Mostafa M. Elbadawi^{a, b, *}, Wagdy M. Eldehna^b, Wenjie Wang^c, Keli K. Agama^c, Yves Pommier^c, Manabu Abe^{a, **}

^a Department of Chemistry, Graduate School of Science, Hiroshima University, 1-3-1 Kagamiyama, Higashi-Hiroshima, Hiroshima, 739-8526, Japan

^b Department of Pharmaceutical Chemistry, Faculty of Pharmacy, Kafrelsheikh University, Kafrelsheikh, 33516, Egypt

^c Developmental Therapeutics Branch & Laboratory of Molecular Pharmacology, Center for Cancer Research, National Cancer Institute, NIH, Bethesda, MD, USA

ARTICLE INFO

Article history:

Received 10 October 2020

Received in revised form

11 January 2021

Accepted 28 January 2021

Available online 9 February 2021

Keywords:

Regioselectivity

Synthesis

Quinoline

Anticancer

Topoisomerase I

ABSTRACT

In our attempt to develop potential anticancer agents targeting Topoisomerase I (TOP1), two novel series of 4-alkoxy-2-arylquinolines **14a-p** and **19a-c** were designed and synthesized based on structure activity relationships of the reported TOP1 inhibitors and structural features required for stabilization of TOP1-DNA cleavage complexes (TOP1ccs). The *in vitro* anticancer activity of these two series of compounds was evaluated at one dose level using NCI-60 cancer cell lines panel. Compounds **14e-h** and **14m-p**, with *p*-substituted phenyl at C2 and propyl linker at C4, were the most potent and were selected for assay at five doses level in which they exhibited potent anticancer activity at sub-micromolar level against diverse cancer cell lines. Compound **14m** was the most potent with full panel GI₅₀ MG-MID 1.26 μM and the most sensitive cancers were colon cancer, leukemia and melanoma with GI₅₀ MG-MID 0.875, 0.904 and 0.926 μM, respectively. Melanoma (LOX IMVI) was the most sensitive cell line to all tested compounds displaying GI₅₀ from 0.116 to 0.227 μM, TGI from 0.275 to 0.592 μM and LC₅₀ at sub-micromolar concentration against almost of the tested compounds. Compounds **14e-h** and **14m-p** were assayed using TOP1-mediated DNA cleavage assay to evaluate their ability to stabilize TOP1ccs resulting in cancer cell death. The morpholino analogs **14h** and **14p** exhibited moderate TOP1 inhibitory activity compared to 1 μM camptothecin suggesting their use as lead compounds that can be optimized for the development of more potent anticancer agents with potential TOP1 inhibitory activity. Finally, Swiss ADME online web tool predicted that compounds **14h** and **14p** possessed good oral bioavailability and druglikeness characteristics.

© 2021 Elsevier Masson SAS. All rights reserved.

1. Introduction

Worldwide, cancer is considered as one of the leading health complications with remarkable increases in the number of patients annually, which is expected to rise to 21.6 million cases in 2023 compared with 14.1 million in 2012 [1,2]. Based on 2018 global

cancer statistics, 18.1 million new cases and 9.8 million cancer deaths were estimated. Lung cancer is the most common cancer diagnosed representing 11.6% of all cases and is the leading cause of cancer death with a mortality rate of 18.4%, followed by breast cancer with incidence 11.6% and mortality 6.6%, then colorectal cancer with incidence and mortality 10.2% and 9.2%, respectively. The incidence and mortality of cancer are fast growing and cancer is expected to be the leading cause of death in the 21st century [3]. Consequently, tremendous efforts are being accomplished to develop potent anticancer agents. Among these efforts, the synthesis of compounds with different scaffolds can inhibit potential chemotherapeutic targets resulting in cancer cell death [4–6].

Quinoline is one of the most privileged scaffolds in drug

* Corresponding author. Department of Chemistry, Graduate School of Science, Hiroshima University, 1-3-1 Kagamiyama, Higashi-Hiroshima, Hiroshima, 739-8526, Japan.

** Corresponding author.

E-mail addresses: mostafa_elbadawi@pharm.kfs.edu.eg (M.M. Elbadawi), mabe@hiroshima-u.ac.jp (M. Abe).

discovery playing a prominent role in medicinal chemistry and is considered as the most ubiquitous heterocyclic motif with versatile medicinal applications [7]. Quinoline derivatives were synthesized and investigated in different applications including antimalarial, antibacterial and anticancer activity [8–11]. Strikingly, quinoline scaffold plays a crucial role in anticancer drug discovery and its derivatives have demonstrated exquisite results as anticancer candidates through numerous mechanisms of action including DNA intercalation, inhibition of tubulin polymerization, DNA repair and angiogenesis, in addition to inhibition of different enzymes that are critically involved in the process of cancer growth [8,12–14]. Within these prominent enzymes, quinoline derivatives were found to be inhibitors of EGFR [15–17], VEGFR [12], carbonic anhydrase enzyme [18], Pim-1 kinase [19], histone deacetylase [20], c-Met factor [21] and preferentially topoisomerase I enzyme [22–24].

Topoisomerase I (TOP1) is a ubiquitous nuclear enzyme and is essential in different cellular processes like replication and transcription. TOP1 relaxes the supercoiled DNA by nicking a single DNA strand through transesterification reaction using Tyr723 in the TOP1 active site which attacks DNA at 3'-phosphodiester end forming 3'-phosphotyrosine covalent linkage allowing the cleaved strand to freely rotate around the intact one solving all topological problems of DNA resulting from replication and transcription. After DNA relaxation, the 5'-hydroxyl end of the broken DNA strand will reverse the 3'-phosphotyrosyl linkage resulting in DNA rejoining and liberation of TOP1. Normally, the binary TOP1-DNA cleavage complexes (TOP1ccs) are transient and not detectable, since the rejoining process is favored [25–30]. Rapidly dividing cancer cells have overexpressed levels of TOP1 and compromised DNA repair which demonstrate the increased sensitivity of cancer cells to TOP1 inhibitors. So, TOP1 is considered an effective and validated chemotherapeutic target for cancer treatment [31–34].

TOP1 inhibitors reversibly bind at the interface of TOP1ccs by stacking hydrophobic interactions with the base pairs flanking the TOP1-mediated cleavage site, besides the hydrogen bonding with TOP1 residues. As a result, TOP1 inhibitors slow down the rejoining process of the scissile DNA, causing replication fork and transcription complex collision with ternary TOP1-drug-DNA complexes resulting in irreversible TOP1ccs which lead to double strand breaks and cell death. Hence, TOP1 inhibitors that stabilize TOP1ccs are known as TOP1 poisons [27,35]. TOP1 poisons are among the most commonly used and effective anticancer agents which are eligible as targeted therapies due to their exquisite selectivity [28].

Camptothecin **1** and its FDA approved derivatives; topotecan **2** and irinotecan **3** (Fig. 1) are TOP1 poisons [33,36]. Unfortunately, the clinical use of topotecan **2** and irinotecan **3** as anticancer drugs has been hampered due to several drawbacks including metabolic instability due to hydrolysis of the essential lactone ring at physiological pH, dose-limiting toxicity with myelosuppression and severe diarrhea, poor water solubility and drug efflux-induced clinical resistance. Therefore, enormous efforts have been established to develop better TOP1 poisons [5,37,38]. Meanwhile, it has been challenging to overcome camptothecins (CPTs) metabolic instability by simple semisynthetic modifications as the lactone ring is essential for TOP1ccs binding interactions. Subsequently, indenoisoquinolines were developed as non-CPT TOP1 poisons by NCI through screening of drug database for compounds with cytotoxicity profiles correlated with CPTs. These indenoisoquinolines offer diverse advantages over CPTs including chemical stability, more stable ternary TOP1ccs, undetectable drug efflux-mediated resistance and targeting TOP1 at different genomic sites [28]. Interestingly, some of indenoisoquinolines succeeded to enter phase I clinical trials for treatment of lymphomas and solid tumors like indotecan (LMP400) **4**, indimitecan (LMP776) **5**, LMP744 **6**.

Moreover, dibenzonaphthyridinones Genz-644282 **7** and ARC-111 **8** have good TOP1-targeting activity as the indenoisoquinolines and are well tolerated in phase I clinical trials (Fig. 1) [28,32,38,39] and in PDX models [40]. There are some evidences that TOP1 inhibitors can target specific cancer cell genes more selectively than others. Thus, extensive efforts have been made to develop novel TOP1 inhibitors with different scaffolds based on the structural requirements of the reported TOP1 poisons aiming to discover promising anticancer agents with better activity and reduced side effects [24,38,40–44].

Based on those previous findings, we herein report the rational design and regioselective synthesis of two series of 4-alkoxy-2-arylquinolines **14a-p** and **19a-c** as potential anticancer agents that can trap TOP1ccs. These lead compounds can be optimized to develop a novel class of potent TOP1 poisons. The design strategy is depicted in Fig. 2. It is based on the structural features of the reported CPTs and non-CPT TOP1 poisons **1–8** (Fig. 1). From the crystal structures of TOP1 poisons ternary complexes, it was revealed that the polycyclic flat planar ring structure is essential to intercalate and stack on the base pairs at the TOP1-induced cleavage site, stabilizing the ternary complex and hindering DNA rejoining. In addition, a hydrogen bond acceptor to project into the minor groove and form hydrogen bonding with the sole amino acid residue in this site; Arg364 [26]. For our design, we selected quinoline core mimicking CPTs **1–3**, Genz-644282 **7** and ARC-111 **8**. For substitutions, we anticipated that the presence of aryl substituent at C2 of quinoline would impart the required polycyclic structure suitable for the intercalation. Furthermore, N1 or O at C4 may be positioned to form a hydrogen bond with Arg364. Also, it was found that the alkyl amino side chain with heteroatom found in indenoisoquinolines **4–6** and dibenzonaphthyridinones **7, 8** serve as hydrogen bond acceptor with Asn352 or Glu356 located in the major groove of the ternary complex [24]. Hence, we assumed that the alkyl amino incorporated at C4 position of 2-arylquinoline will project towards the residues in the major groove acting as a hydrogen bond acceptor. Moreover, we conserved the two methoxy groups at C6 and C7 like TOP1 poisons **4–6**, which are reported to hydrogen bond with Asn722 in one of the binding pockets of the major groove [27]. In order to study the impact of substitution pattern on the anticancer activity and TOP1 inhibitory activity, we introduced alkyl chain with different length and different heterocyclic amines at C4, in addition to different aryl substituents at C2 position.

The designed compounds were synthesized and evaluated for *in vitro* anticancer activity according to NCI-60 cancer cell lines screening protocol, then the most promising anticancer agents were evaluated for TOP1 inhibitory activity using TOP1-mediated DNA cleavage assays. From this study, we obtained several compounds with promising anticancer activity **14e-h** and **14m-p** and some of them **14h** and **14p** stabilized TOP1ccs. To the best of our knowledge, this is the first study that reports on 4-alkoxy-2-arylquinolines as topoisomerase I inhibitors. Thus, in our future study we will optimize these TOP1 poisons lead compounds to afford more potent candidates.

2. Results and discussion

2.1. Chemistry

The synthetic routes used for preparation of the two series of target 4-alkoxy-2-arylquinolines **14a-p** and **19a-c** are depicted in Schemes 1 and 2, respectively. The 2-aminoacetophenone derivative **9** was converted to the benzoyl derivatives **11a, b** in excellent yields (81–85%) by reaction with the appropriate benzoyl chloride **10a, b** in the presence of Et₃N as a base in dry THF at 0 °C followed

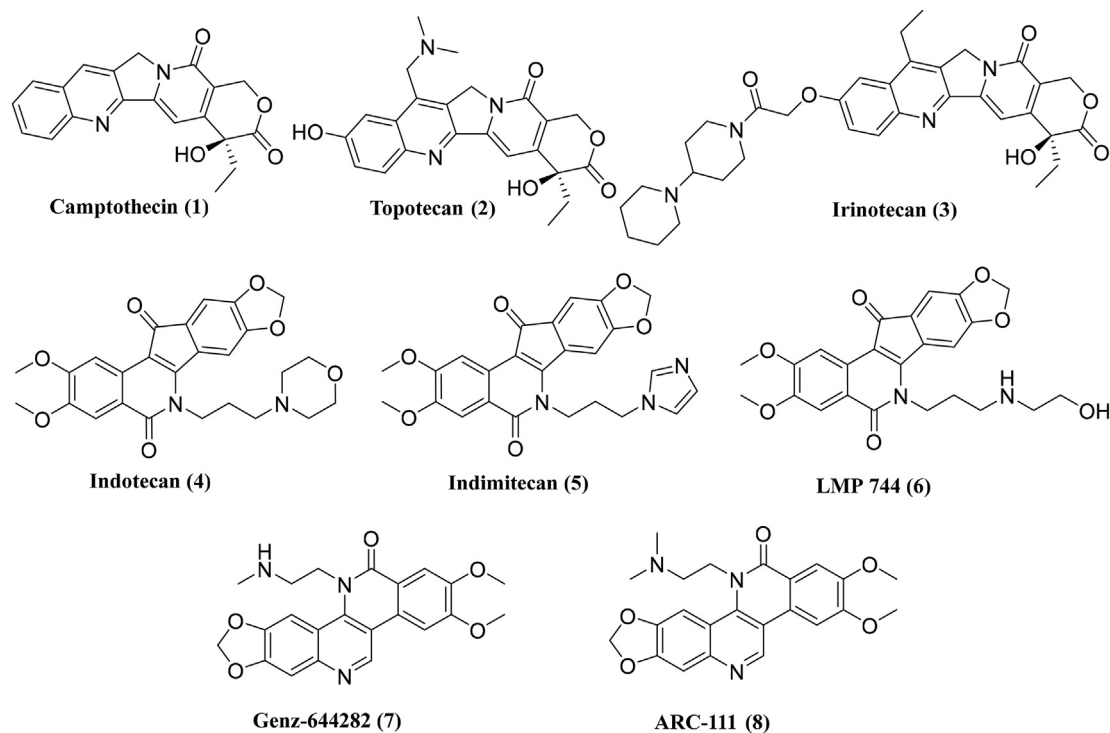


Fig. 1. TOP1 inhibitors; camptothecins (1–3) and in clinical trials (4–8).

by stirring at room temperature [45,46]. Then, the benzoyl derivatives **11a, b** were cyclized under nitrogen using aldol condensation reaction in refluxing dry dioxane and sodium hydroxide to afford the quinolones **12a, b** in 91% and 90% yields, respectively [47]. The *O*-alkylated regioisomers **13a–d** were prepared by stirring of quinolones **12a** or **12b** with excess KOH and catalytic amount of KI in dry DMF for 2 h, then the produced nucleophile was reacted with the respective 1-bromo-2-chloroethane or 1-bromo-3-chloropropane for 24 h at room temperature to obtain the key intermediates **13a–d** in good to excellent yields (78–89%) [48].

The quinolones **12a, b** are ambident anions and *O*- versus *N*-regioselectivity differs within the same scaffold based on temperature, substituents, solvent and nature of the electrophiles, so we had to confirm *O*-regioselectivity of the synthesized key intermediates **13a–d** to be more confident in understanding the structure activity relationships of the final products especially, it was reported that regio-inaccurate structures are present in compound collections even for starting materials available to purchase from vendors [49–51]. One dimensional (1D) NMR alone is not enough for this confirmation, so we utilized FTIR spectroscopy besides the reported NMR-based strategy which depends on using two dimensional (2D) NMR: $^1\text{H}-^{13}\text{C}$ HSQC, $^1\text{H}-^{13}\text{C}$ HMBC and $^1\text{H}-^1\text{H}$ NOESY [49]. 2D NMR spectra for the representative key intermediate **13a** are illustrated in Fig. 3. Regarding FTIR spectrum, carbonyl stretching band appeared at 1683 cm^{-1} for the quinolone starting material **12a**, while this band disappeared in **13a** after alkylation which confirmed *O*-alkylation. Furthermore, HSQC demonstrated H9/C9 crosspeak that provided the chemical shifts for C9 and H9 neighboring to the alkylation site, in addition H9/C4 correlation was observed in HMBC spectrum which concluded that H9 must be within three atoms of C4 and this correlation pattern impossible in *N*-alkyl analog. Moreover, the data from NOESY displayed a crosspeak between H3 and H9 which means that H3 is close to H9. Consequently, we can confirm that the synthesized key intermediates **13a–d** are *O*-regioisomers.

Finally, the key intermediates **13a–d** were converted to the target 4-alkoxy-2-arylquinolines **14a–p** in good to excellent yields (63–92%) by nucleophilic substitution reaction with different alicyclic amines in dry DMF in the presence of anhydrous K_2CO_3 as a base at $90\text{ }^\circ\text{C}$ [48]. Similarly, syntheses of the second series of the target 4-alkoxy-2-arylquinolines **19a–c** (Scheme 2) were accomplished using the same procedures for the first series. The structures of all synthesized compounds were confirmed using 1D and 2D NMR (see supplementary data for 2D NMR), FTIR spectroscopy, high resolution mass spectrometry (HRMS) and single crystal X-ray crystallography for one of the final compounds **14b**.

2.2. Single crystal X-ray crystallography

For more certainty of structure elucidation, a single crystal X-ray crystallography for one of the target 4-alkoxy-2-arylquinolines **14b** was conducted, Fig. 4. Crystals of compound **14b** were obtained by slow evaporation of its solution in chloroform. The crystals were measured using Bruker APEX-II D8 diffractometer with monochromatic Mo $K\alpha$ diffraction radiation type ($\lambda = 0.71073\text{ \AA}$) at 90 K as ambient temperature. Structure refinement was conducted by SHELXL. Crystallographic data for compound **14b** have been deposited at Cambridge Crystallographic Data Center and given the deposition number: CCDC 2023795. The crystallographic data and refinement are available in the supplementary data. Regarding the X-ray structure of compound **14b**, we can assert the *O*-regioselectivity of the target 4-alkoxy-2-arylquinolines under the conditions were utilized, thus we can attain more confident study of structure activity relationships.

2.3. In vitro anticancer activity

The structures for the synthesized 4-alkoxy-2-arylquinolines **14a–p** and **19a–c** were submitted to the Developmental Therapeutics Program (DTP) of the National Cancer Institute (NCI) (www.dtp).

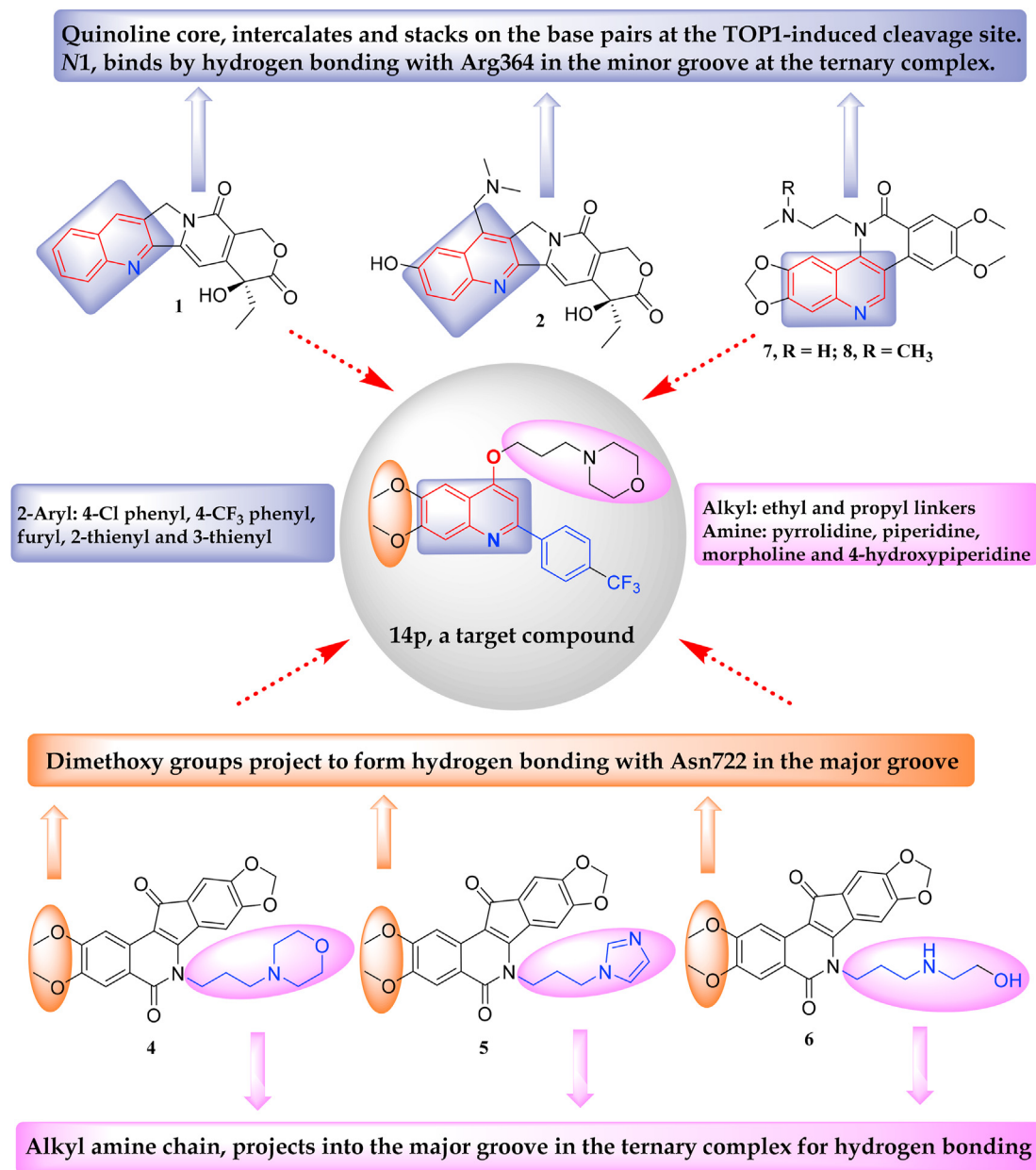


Fig. 2. Rational design for the target compounds generated from the reported TOP1 inhibitors.

nci.nih.gov). All compounds were selected for NCI-60 human cancer cell lines screening for their *in vitro* anticancer activity [52,53].

2.3.1. Preliminary cytotoxicity screening at 10 μ M concentration

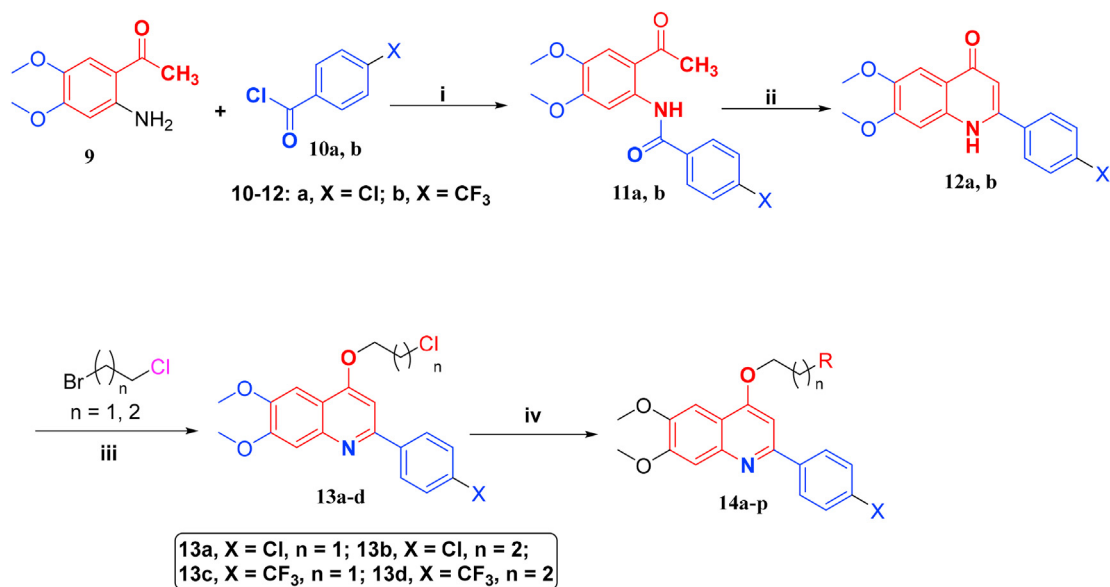
Firstly, the selected 4-alkoxy-2-arylquinolines **14a-p** and **19a-c** were screened for anticancer activity at a dose of 10 μ M against a panel of 59 cancer cell lines representing nine cancer types: leukemia, lung, colon, CNS, melanoma, ovarian, renal, prostate and breast cancers. The sulforhodamine B (SRB) assay was used to determine the growth and cell viability [54]. The mean % growth inhibition values (GI%) for compounds **14a-p** and **19a-c** against NCI-59 cancer cell lines full panel are depicted in Fig. 5.

Concerning the cytotoxicity screening at 10 μ M, compounds **14a-d** bearing ethyl linker at C4 position and *p*-chlorophenyl at C2 position demonstrated low anticancer activity with GI% = 3–17%. The replacement of chloro in **14a-d** with CF₃ substituent in **14i-l** slightly enhanced the anticancer activity displaying GI% = 13–34%.

Interestingly, 4-alkoxy-2-arylquinolines with propyl linker at C4 and *p*-chlorophenyl at C2 **14e-h** exhibited significant improvement in the growth inhibitory activity with GI% = 62–65% compared to **14a-d** with ethyl linker. Similarly, the replacement of chloro in compounds **14e-h** with CF₃ substituent in **14m-p** enhanced the anticancer activity affording the most potent counterparts in these series. Conversely, the biosteric replacement of *p*-substituted phenyl at C2 with 2-furyl, 2-thienyl and 3-thienyl in **19a-c** significantly reduced the anticancer activity demonstrating GI% = 46, 20 and 32%, respectively. Consequently, utilizing a propyl linker at C4 and appending a *p*-substituted phenyl moiety at C2 are suggested to be crucial elements for the anticancer activity for the herein reported 4-alkoxy-2-arylquinolines.

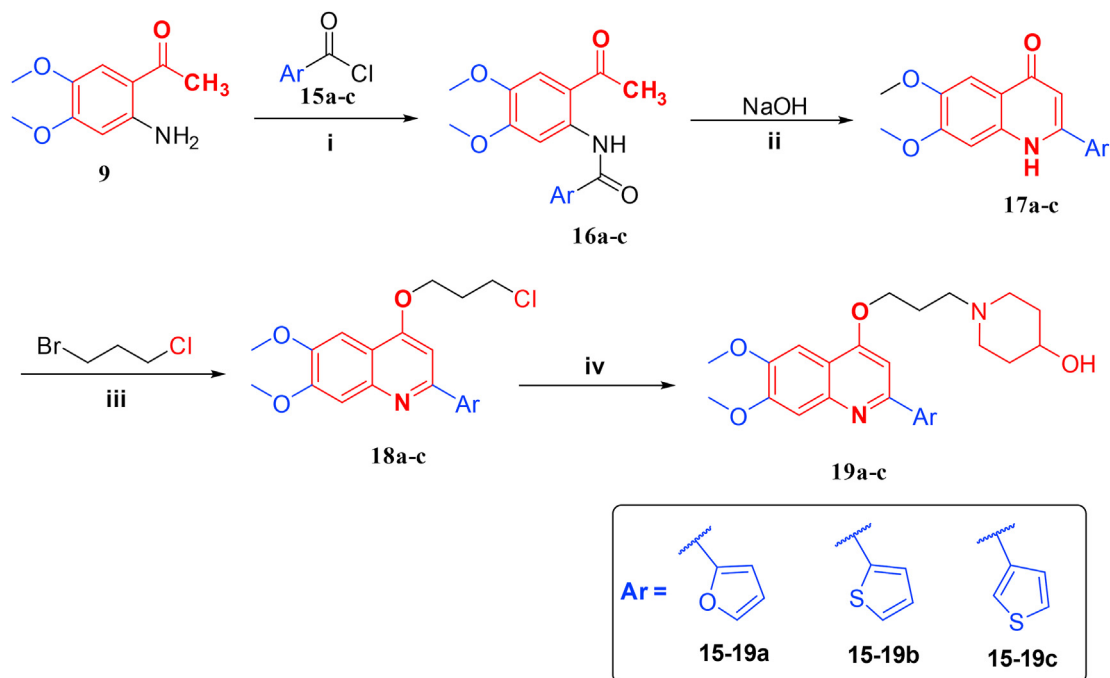
2.3.2. *In vitro* cytotoxicity evaluation against NCI-59 cancer cell lines panel at five doses level

Based on the preliminary screening at 10 μ M, propyl linker-



14	X	n	R	14	X	n	R	14	X	n	R
a	Cl	1	Pyrrolidine	g	Cl	2	Piperidine	m	CF ₃	2	Pyrrolidine
b	Cl	1	4-Hydroxypiperidine	h	Cl	2	Morpholine	n	CF ₃	2	4-Hydroxypiperidine
c	Cl	1	Piperidine	i	CF ₃	1	Pyrrolidine	o	CF ₃	2	Piperidine
d	Cl	1	Morpholine	j	CF ₃	1	4-Hydroxypiperidine	p	CF ₃	2	Morpholine
e	Cl	2	Pyrrolidine	k	CF ₃	1	Piperidine				
f	Cl	2	4-Hydroxypiperidine	l	CF ₃	1	Morpholine				

Scheme 1. Synthesis of target 4-alkoxy-2-arylquinolines **14a-p**; Reagents and conditions: (i) Et₃N, THF, 0 °C then rt, overnight; (ii) NaOH, dry dioxane, 110 °C under N₂, 4 h; (iii) KOH, KI, alkyl halide, dry DMF, rt, 24 h; (iv) KI, anhydrous K₂CO₃, amine, dry DMF, reflux, 12 h.



Scheme 2. Synthesis of target 4-alkoxy-2-arylquinolines **19a-c**; Reagents and conditions: (i) Et₃N, THF, 0 °C then rt, overnight; (ii) NaOH, dry dioxane, 110 °C under N₂, 4 h; (iii) KOH, KI, 1-bromo-3-chloropropane, dry DMF, rt, 24 h; (iv) KI, anhydrous K₂CO₃, 4-hydroxypiperidine, dry DMF, reflux, 12 h.

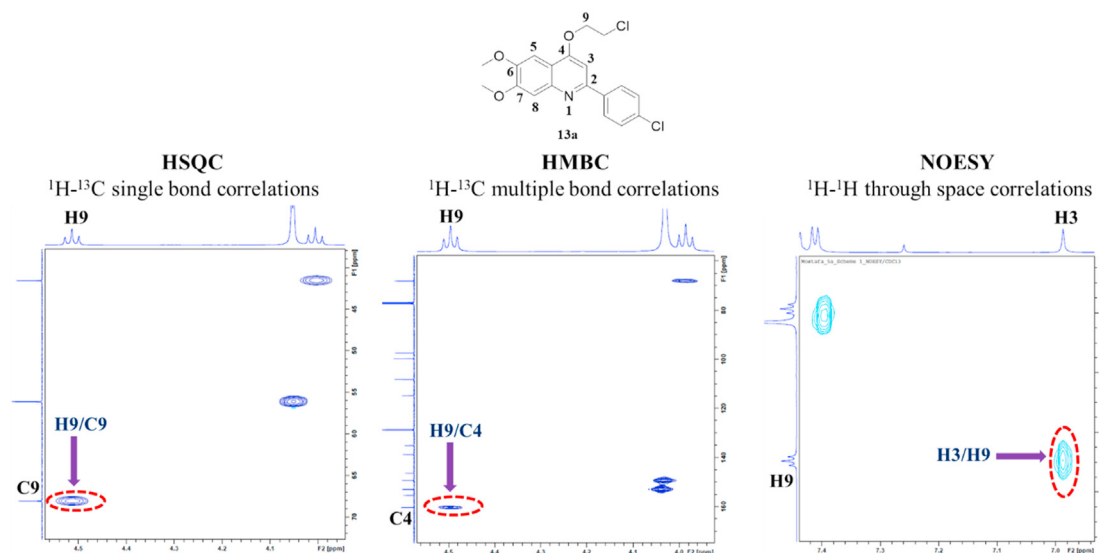


Fig. 3. 2D NMR spectra of compound **13a**: ^1H - ^{13}C HSQC, ^1H - ^{13}C HMBC and ^1H - ^1H NOESY.

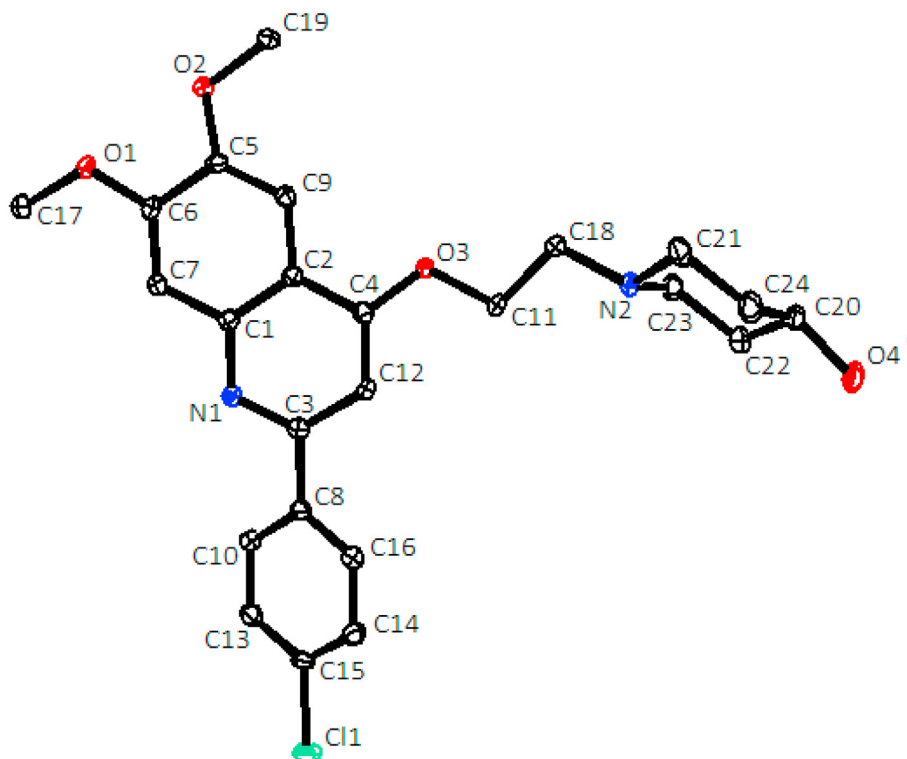


Fig. 4. The ORTEP diagram of the final X-ray structure of compound **14b**.

bearing 2-arylquinolines **14e-h** and **14m-p** exhibited significant growth inhibition against various cancer cell lines representing different cancer types. Therefore, these compounds were selected by NCI for further examination at five doses level (0.01–100 μM). Three dose response parameters were calculated: GI_{50} , TGI and LC_{50} .

Regarding the whole panel of cancer cell lines, compound **14m** displayed the best potent anticancer activity against the entire panel of cancer cell lines with GI_{50} values range 0.116–6.77 μM exhibiting GI_{50} at sub-micromolar concentration over 28 tumor cell

lines. In this regard, the most sensitive cell lines were leukemia (SR), non-small cell lung cancer (NCI-H226), colon cancer (COLO205), CNS cancer (SF-295), melanoma (LOX IMVI, SK-MEL-5), ovarian cancer (NCI/ADR-RES), renal cancer (CAKI-1) and breast cancer (T-47D) with GI_{50} values = 0.133, 0.343, 0.401, 0.328, 0.116, 0.247, 0.458, 0.188 and 0.472 μM , respectively (Table 1). Concerning the sensitivity against all cancer cell lines, compound **14m** possessed significant antiproliferative activity with full panel GI_{50} MG-MID 1.26 μM and cancer subpanels GI_{50} MG-MID range 0.875–1.70 μM possessing superior activity at sub-micromolar level

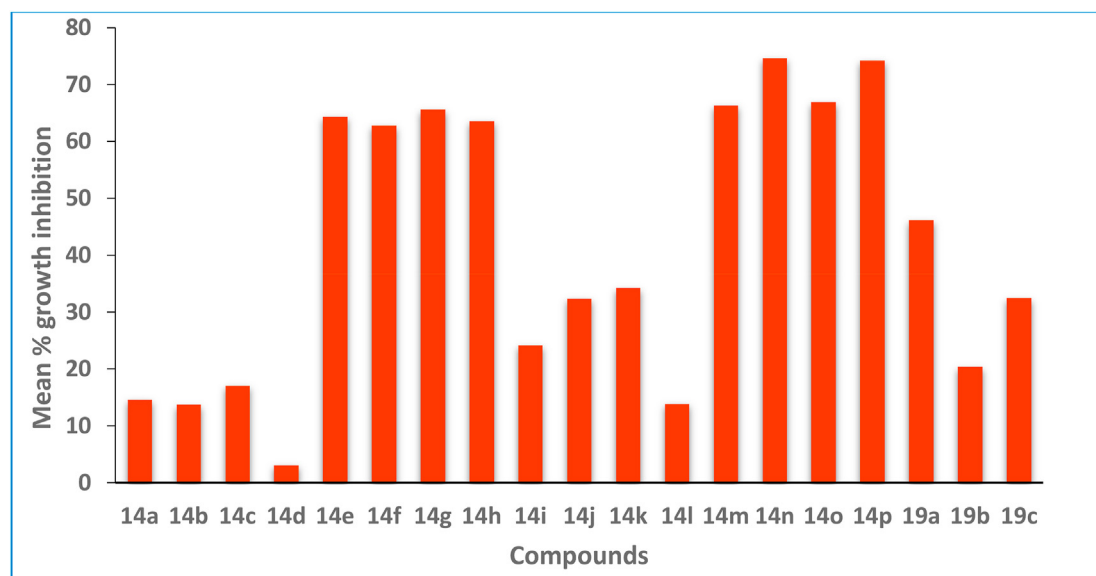


Fig. 5. Mean % growth inhibition of compounds **14a-p** and **19a-c** against NCI 59 cancer cell line panel.

against colon cancer, then leukemia and melanoma cells with subpanel GI_{50} MG-MID values 0.875, 0.904 and 0.926 μM , respectively (Table 2). In addition, compound **14m** displayed significant cytostatic effect over different cell lines with full panel TGI MG-MID = 11.61 μM (Table 3) and TGI values $\leq 5 \mu\text{M}$ against 18 cancer cell lines, among them melanoma (LOX IMVI and SK-MEL-5) with TGI 0.275 and 0.645 μM , respectively (see supplementary data for details of TGI values). Besides, it was found that **14m** proved to have a lethal effect against melanoma (LOX IMVI) with LC_{50} 0.656 μM (see supplementary data for details of LC_{50} values) and melanoma LC_{50} MG-MID 23.7 μM (Table 3).

Similarly, compound **14o** exhibited significant anticancer potential in the second order showing GI_{50} range from 0.162 to 8.70 μM and values at sub-micromolar concentration against 24 cancer cell lines. From these cell lines, the most sensitive were leukemia (SR), non-small cell lung cancer (NCI-H226), colon cancer (HCT-15 and COLO205), melanoma (LOX IMVI, SK-MEL-5 and M14), renal cancer (CAKI-1) and breast cancer (T-47D) demonstrating GI_{50} values = 0.193, 0.370, 0.399, 0.406, 0.162, 0.325, 0.327, 0.272 and 0.454 μM , respectively (Table 1). In regard of the influence on the whole panel of cancer cell lines, compound **14o** showed considerable anti-proliferative activity displaying full panel GI_{50} MG-MID 1.57 μM with subpanels GI_{50} MG-MID from 1.13 to 2.13 μM . Breast cancer and melanoma cells were the most affected ones with GI_{50} MG-MID 1.13 and 1.19 μM , respectively (Table 2). In the concern of cytostatic potential, compound **14o** has established advantageous effect with full panel TGI MG-MID = 11.58 μM (Table 3) and TGI values $\leq 5 \mu\text{M}$ against 14 tumor cell lines and the most sensitive ones were melanoma (LOX IMVI and SK-MEL-5) with TGI 0.355 and 1.20 μM , respectively (supplementary data). Also, compound **14o** had good lethal activity on melanoma (LOX IMVI) expressed as LC_{50} = 0.779 μM (supplementary data) and melanoma LC_{50} MG-MID = 19.9 μM (Table 3).

In a similar manner, compound **14e** demonstrated excellent anticancer effect in the third order with GI_{50} range 0.191–3.36 μM against the whole panel of tumor cell lines showing GI_{50} values at sub-micromolar level over 16 different cell lines. It was established that leukemia (SR), colon cancer (HT29, COLO205), melanoma (LOX IMVI and M14) and renal cancer (CAKI-1) were the most susceptible cell lines with GI_{50} equal 0.251, 0.454, 0.459, 0.191, 0.402 and

0.303 μM , respectively (Table 1). In the context of activity over the entire panel cell lines, compound **14e** exerted remarkable anticancer potential with full panel GI_{50} MG-MID 1.65 μM and cancer subpanels GI_{50} MG-MID ranged from 1.36 to 2.14 μM with values 1.36 and 1.37 μM for the most susceptible breast and colon cancers, respectively (Table 2). Furthermore, compound **14e** established comparable cytostatic influence for various cell lines with full panel TGI MG-MID = 8.71 μM (Table 3) and TGI values $\leq 5 \mu\text{M}$ over 19 cancer cell lines, preferably melanoma (LOX IMVI) with TGI = 0.446 μM (supplementary data). Moreover, compound **14e** exerted lethal impact against melanoma (LOX IMVI) with LC_{50} = 1.12 μM (supplementary data) and melanoma LC_{50} MG-MID equals 14.6 μM (Table 3).

In a similar fashion, compounds **14f**, **g** and **h** have exerted good anticancer impact over the entire panel of cancer cells with GI_{50} ranges 0.227–4.27, 0.189–3.85 and 0.217–3.87 μM , respectively, showing GI_{50} values at sub-micromolar level for 11, 13 and 11 cancer cell lines, respectively. For compound **14f**, leukemia (SR), melanoma (LOX IMVI) and renal cancer (CAKI-1) were the most sensitive with GI_{50} = 0.373, 0.227 and 0.416 μM , respectively, and the same sensitivity has been noticed for compounds **14g** and **14h** exhibiting GI_{50} values 0.373, 0.189 and 0.287 μM for **14g**, while GI_{50} = 0.414, 0.217 and 0.305 μM for **14h**, respectively. In addition, melanoma (M14) and colon cancer (HT29) showed preferred sensitivity to **14g** with GI_{50} = 0.412 and 0.492 μM , respectively (Table 1). Concerning the sensitivity against all cancer cell lines, compounds **14f**, **g** and **h** had favorable anticancer effectiveness with full panel GI_{50} MG-MID = 1.99, 1.83 and $> 3.29 \mu\text{M}$ and tumor subpanels GI_{50} MG-MID ranges 1.50–2.51, 1.54–2.30 and 1.40 – $>13.90 \mu\text{M}$, respectively (Table 2). Melanoma and colon cancer were the most sensitive to **14f** and **14g** with GI_{50} MG-MID 1.50 and 1.65 μM for **14f** and 1.54 and 1.57 μM for **14g**, respectively, while melanoma and renal cancer were the most susceptible for **14h** with GI_{50} MG-MID 1.40 and 1.66 μM , respectively (Table 2). Moreover, compounds **14f**, **g** and **h** have exerted good cytostatic action against diverse cancer cell lines with TGI $\leq 5 \mu\text{M}$ over 18, 16 and 7 cancer cell lines, respectively, demonstrating melanoma (LOX IMVI) as the most affected cell line with TGI = 0.589, 0.435 and 0.592 μM , respectively (supplementary data). While, Compounds **14f**, **h** displayed lethal impact on melanoma (LOX IMVI) with LC_{50} = 2.20,

Table 1
GI₅₀ values of NCI *in vitro* cytotoxicity testing of compounds **14e-h** and **14m-p** at five doses level.^{a,b}

Panel/cancer cell lines	Compounds							
	14e	14f	14g	14h	14m	14n	14o	14p
	GI ₅₀ (μM)							
Leukemia								
CCRF-CEM	2.14	2.65	2.79	3.35	1.08	3.26	1.83	2.79
HL-60(TB)	2.72	4.27	NT	NT	1.84	13.9	2.91	9.58
K-562	1.06	1.63	1.22	2.71	0.475	1.79	0.578	1.18
MOLT-4	1.50	1.80	2.04	2.85	0.994	3.27	1.70	2.51
SR	0.251	0.373	0.373	0.414	0.133	0.274	0.193	0.242
Non-small cell lung cancer								
A549/ATCC	1.52	2.20	1.90	2.02	0.653	1.65	0.722	1.04
EKVX	1.21	1.33	1.47	1.73	0.982	1.03	0.803	1.61
HOP-62	1.38	1.98	2.37	1.98	1.03	1.80	0.947	1.67
HOP-92	0.850	1.25	1.02	1.36	0.460	1.68	0.678	1.00
NCI-H226	0.898	1.39	1.12	0.997	0.343	1.59	0.370	0.406
NCI-H23	2.45	2.83	2.95	NT	1.91	6.16	1.91	2.36
NCI-H322 M	3.36	3.22	4.42	>100	6.77	10.2	8.70	10.5
NCI-H460	0.823	0.955	0.842	0.958	0.528	0.835	0.595	0.639
NCI-H522	2.36	2.19	3.28	2.17	1.74	4.15	2.44	2.52
Colon Cancer								
COLO205	0.459	0.532	0.582	0.620	0.401	0.456	0.406	0.529
HCC-2998	1.86	1.95	2.34	1.97	1.45	4.07	1.28	1.41
HCT-116	0.699	1.44	0.828	1.59	0.456	0.671	0.429	0.583
HCT-15	0.567	0.763	0.604	0.754	0.416	0.667	0.399	0.520
HT29	0.454	0.700	0.492	0.610	0.446	0.486	0.415	0.540
KM12	2.46	3.13	3.07	3.87	1.34	6.87	2.92	3.42
SW-620	3.12	3.05	3.09	3.57	1.62	3.53	2.91	3.51
CNS Cancer								
SF-268	2.53	3.36	3.20	NT	2.39	5.76	3.76	5.7
SF-295	1.22	1.66	1.21	1.08	0.328	1.61	0.530	0.349
SF-539	2.44	2.28	2.57	2.99	1.87	5.75	2.08	3.18
SNB-19	3.14	3.19	2.98	NT	2.77	10.5	2.82	2.91
SNB-75	1.73	1.76	1.98	2.06	1.85	2.58	1.96	2.46
U251	1.79	2.81	1.89	1.92	1.05	2.12	1.10	1.40
Melanoma								
LOX IMVI	0.191	0.227	0.189	0.217	0.116	0.190	0.162	0.141
MALME-3M	1.68	1.89	1.74	2.01	1.01	2.65	1.26	1.38
M14	0.402	0.591	0.412	0.545	0.336	0.535	0.327	0.355
MDA-MB-435	2.72	2.05	2.44	1.90	0.709	2.76	1.23	1.20
SK-MEL-2	2.16	2.07	2.75	NT	1.93	3.85	2.64	3.32
SK-MEL-28	1.48	1.49	1.45	1.52	1.20	2.38	1.26	1.44
SK-MEL-5	0.961	1.27	1.10	0.832	0.247	1.43	0.325	0.288
UACC-257	1.96	2.06	1.92	1.92	1.41	2.28	1.70	1.67
UACC-62	2.03	1.90	1.94	2.26	1.38	2.61	1.82	0.628
Ovarian Cancer								
IGROV1	0.881	0.923	0.838	0.990	0.592	0.900	0.651	0.830
OVCAR-3	2.71	3.24	3.23	NT	2.15	6.10	2.44	3.73
OVCAR-4	3.00	4.34	3.85	NT	3.71	9.14	2.91	10.3
OVCAR-5	1.03	1.16	1.16	1.58	0.803	3.14	0.710	1.92
OVCAR-8	1.19	2.00	1.77	2.15	0.806	1.66	0.734	1.95
NCI/ADR-RES	0.683	0.925	0.898	1.15	0.458	0.847	0.522	0.640
SK-OV-3	2.42	3.17	NT	3.00	2.55	10.6	2.30	5.04
Renal Cancer								
786-0	2.78	3.31	2.62	1.94	2.13	4.72	2.17	1.76
A498	2.19	1.52	1.40	1.59	1.58	2.37	1.85	1.51
ACHN	1.93	2.43	2.45	3.64	0.812	3.18	1.20	2.01
CAKI-1	0.303	0.416	0.287	0.305	0.188	0.376	0.272	0.167
RXF 393	1.17	1.22	1.08	1.12	1.13	1.34	1.09	0.706
SN 12C	0.914	1.26	0.946	1.30	0.673	1.44	0.668	0.675
TK-10	2.33	2.14	3.73	NT	3.24	11.5	7.80	13.9
UO-31	1.72	1.72	1.87	1.78	2.02	2.71	2.00	1.77
Prostate Cancer								
PC-3	1.76	2.02	1.74	2.63	1.07	3.66	1.34	2.19
DU-145	2.15	2.78	2.54	NT	1.37	4.96	1.84	10.1
Breast Cancer								
MCF7	1.33	1.60	1.56	2.49	0.976	2.57	1.16	1.55
MDA-MB-231/ATCC	0.907	0.665	0.666	1.01	0.565	0.919	0.536	0.498
HS 578T	1.89	1.91	2.11	2.40	1.74	3.75	2.15	2.25
BT-549	1.77	2.79	1.43	2.59	1.99	6.59	1.48	5.00
T-47D	1.02	2.26	1.31	1.96	0.472	2.97	0.454	0.654
MDA-MB-468	1.28	1.56	1.39	1.83	0.885	1.63	1.03	1.24

^a Bold figure indicates GI₅₀ value at sub-micromolar level.

^b NT = not tested.

Table 2
GI₅₀ mean-graph midpoint (MG-MID)^a of subpanel cancer cell lines for compounds **14e-h** and **14m-p**.

Subpanel cancer cell lines	Compounds							
	14e	14f	14g	14h	14m	14n	14o	14p
	GI ₅₀ MG-MID (μM)							
Leukemia	1.53	2.14	1.60	2.33	0.904^b	4.49	1.44	3.26
Non-small cell lung cancer	1.65	1.92	2.15	>13.90	1.60	3.23	1.90	2.41
Colon cancer	1.37	1.65	1.57	1.85	0.875	2.39	1.25	1.50
CNS cancer	2.14	2.51	2.30	2.01	1.70	4.72	2.04	2.66
Melanoma	1.50	1.50	1.54	1.40	0.926	2.07	1.19	1.15
Ovarian cancer	1.70	2.25	1.95	1.77	1.58	4.26	1.46	3.48
Renal cancer	1.66	1.75	1.79	1.66	1.47	3.45	2.13	2.81
Prostate cancer	1.95	2.4	2.14	2.63	1.22	4.31	1.59	6.14
Breast cancer	1.36	1.79	1.41	2.04	1.10	3.07	1.13	1.86
Full panel GI₅₀ MG-MID^c	1.65	1.99	1.83	>3.29	1.26	3.59	1.57	2.81

^a Median value calculated based on the data from NCI *in vitro* cytotoxicity screening for each cancer type cell lines.

^b GI₅₀ full panel mean-graph midpoint (MG-MID) is the average of GI₅₀ values against all cancer cell lines.

^c Bold figure indicates MG-MID value at sub-micromolar level.

Table 3
TGI and LC₅₀ mean-graph midpoints (MG-MID)^a in μM for the most potent compounds **14e, m** and **o**.

Subpanel cancer cell lines	Compounds					
	14e		14m		14o	
	TGI	LC ₅₀	TGI	LC ₅₀	TGI	LC ₅₀
Leukemia	4.99	32	6.17	81.6	10.29	74.8
Non-small cell lung cancer	10.41	39.7	12.72	57.9	13.79	50.6
Colon cancer	8.31	39.1	8.07	50.4	10.29	40.8
CNS cancer	10.11	33.5	11.71	44.9	11.87	38.8
Melanoma	4.26	14.6	4.08	23.7	4.14	19.9
Ovarian cancer	14.8	55.1	28.1	81	19.67	65.5
Renal cancer	7.66	28.9	10.22	40.1	11.03	35
Prostate cancer	12.05	39.6	16.75	89.5	13.85	42.2
Breast cancer	5.80	29.6	6.80	40.8	9.29	43
Full panel MG-MID^b	8.71	34.67	11.61	56.65	11.58	45.62

^a Median value calculated based on the data from NCI *in vitro* cytotoxicity screening for each cancer type cell lines.

^b Full panel mean-graph midpoint (MG-MID) is the average of TGI or LC₅₀ values against all cancer cell lines.

4.46 μM, respectively, compound **14g** had lethal activity against melanoma (SK-MEL-5) with LC₅₀ = 4.87 μM (supplementary data).

Regarding the anticancer efficacy of compounds **14n** and **14p** against all cancer cell lines, they exhibited a good inhibitory impact on the cell growth at sub-micromolar level against 12 and 9 cancer cell lines with GI₅₀ ranges 0.190–13.9 and 0.141–13.9 μM, respectively (Table 1). For compound **14n**, it was found that leukemia (SR), colon cancer (COLO205 and HT29), melanoma (LOX IMVI) and renal cancer (CAKI-1) were the most sensitive to its anticancer activity with GI₅₀ = 0.274, 0.456, 0.486, 0.190 and 0.376 μM, respectively. While for compound **14p**, leukemia (SR), non-small cell lung cancer (NCI-H226), CNS cancer (SF-295), melanoma (LOXIMVI, M14 and SK-MEL-5), renal cancer (CAKI-1) and breast cancer (MDA-MB-231/ATCC) were the most sensitive with GI₅₀ = 0.242, 0.406, 0.349, 0.141, 0.355, 0.288, 0.167, 0.498 μM, respectively (Table 1). Furthermore, compound **14n** and **14p** had full panel GI₅₀ MG-MID 3.59 and 2.81 μM with tumor subpanels GI₅₀ MG-MID ranges 2.07–4.72 and 1.13–6.14 μM, respectively (Table 2). Notably, melanoma was the most affected cancer to compound **14n** with sub-panel GI₅₀ MG-MID = 2.07 μM, whereas, breast cancer and melanoma were the most sensitive to compound **14p** with GI₅₀ MG-MID = 1.13 and 1.19 μM, respectively (Table 2). Moreover, compounds **14n** and **p** had good cytostatic activity against various

cancer cell lines with TGI ≤5 μM against 4 and 13 tumor cell lines, respectively. Melanoma (LOX IMVI) was the most sensitive cell line to both **14n** and **p** with TGI = 0.447 and 0.324 μM, respectively (supplementary data). In addition, compounds **14n** and **p** displayed lethal effect against melanoma (LOX IMVI) with LC₅₀ 2.13 and 0.747 μM, respectively (supplementary data).

Generally, compound **14m** bearing pyrrolidine moiety and *p*-CF₃ phenyl ring, was the most potent analog against all cancer cell lines with full panel GI₅₀ MG-MID 1.26 μM and the most sensitive cancers were colon cancer, leukemia and melanoma with GI₅₀ MG-MID 0.875, 0.904 and 0.926 μM, respectively (Table 2). It is noteworthy that all the tested compounds **14e-h** and **14m-p** exhibited exquisite growth inhibitory influence on specific cell lines at sub-micromolar level; leukemia (SR), non-small cell lung cancer (NCI-H460), colon cancer (COLO205, HCT-15 and HT29), melanoma (LOX IMVI and M14), ovarian cancer (IGROV1) and renal cancer (CAKI-1) (Table 1). Melanoma (LOX IMVI) was the most sensitive cell line to all compounds **14e-h** and **14m-p** showing GI₅₀ values of 0.191, 0.227, 0.189, 0.217, 0.116, 0.190, 0.162, 0.141 μM, respectively (Table 1). Meanwhile, TGI values were the best for melanoma (LOX IMVI) against all compounds **14e-h** and **14m-p**; 0.446, 0.589, 0.435, 0.592, 0.275, 0.447, 0.355, 0.324 μM, respectively (supplementary data). Also, melanoma (LOX IMVI) was the most susceptible to the lethal effect of **14e, f, h** and **14m-p** displaying LC₅₀ values 1.12, 2.20, 4.46, 0.656, 2.13, 0.779, 0.747 μM, respectively (supplementary data).

With regards to the structure activity relationships, except for **14f**, grafting a *p*-CF₃ substituent at the 2-phenyl ring resulted in a significant enhancement of the overall anticancer activity compared to the *p*-Cl substituent. For chloro analogs **14e-h**, incorporation of pyrrolidine moiety was the most advantageous for anticancer activity, then piperidine, then 4-hydroxypiperidine, then morpholine. While for CF₃ analogs **14m-p**, pyrrolidine was better for anticancer effect, then piperidine, then morpholine, then 4-hydroxypiperidine (Fig. 6).

2.4. Topoisomerase I-mediated DNA cleavage assay

TOP1 poisoning activity of the most potent cytotoxic 4-alkoxy-2-arylquinolines **14e-h** and **14m-p** was investigated using TOP1-mediated DNA cleavage assay which scores the TOP1 poisoning activity of the tested compounds compared to 1 μM camptothecin [28]. The tested compounds at 0.1, 1, 10 and 100 μM were incubated with TOP1 enzyme and 3'-[³²P]-labeled 117-bp DNA oligonucleotide [29]. TOP1 poisons specifically bind to and trap TOP1ccs resulting in stabilization of TOP1ccs and DNA cleavage. The

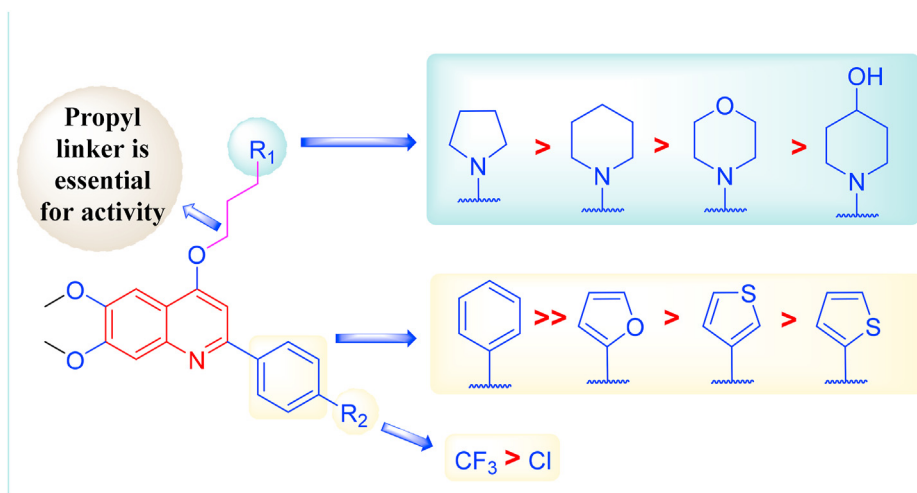


Fig. 6. Summary of structure activity relationships for anticancer activity.

compound-induced trapped TOP1ccs were visualized using gel electrophoresis displaying specific cleavage patterns for each compound in which each gel band represents specific TOP1cc trapped by the drug. Finally, visual comparison of the lanes produced by the tested compounds and that produced by 1 μ M CPT was utilized to give semiquantitative scores to indicate the activity of the tested compounds; 0 (no activity), + (activity between 20 and 50%, the cleavage activity of 1 μ M CPT), ++ (activity between 50 and 75%, the cleavage activity of 1 μ M CPT), +++ (activity between 75 and 100%, the cleavage activity of 1 μ M CPT) and ++++ (activity equipotent to or more potent than 1 μ M CPT) [48,55,56].

From the chloro analogs **14e-h**, compounds **14e-g** exhibited weak TOP1 poisoning activity (+), while compound **14h** displayed moderate activity (++) , Fig. 7. Regarding, CF₃ analogs **14m-p**, compounds **14m, n** displayed no activity (0) and compound **14o** revealed weak activity (+), while compound **14p** exhibited moderate TOP1 inhibitory activity (++) , Fig. 8. From all tested synthesized compounds, compounds **14h, p** bearing morpholine ring, which was found in diverse TOP1 poisons as indotecan (LMP400) **4** in clinical trials, exhibited the best activity with score ++ demonstrating that morpholine ring is preferred for TOP1 inhibitory activity.

Compounds **14h, p** exhibited good anticancer activity at sub-micromolar level against various cancer cell lines and displayed comparable GI₅₀ ranges 0.217–3.87 and 0.141–13.9 μ M, respectively, in addition to the moderate TOP1 poisoning activity leading to DNA cleavage and cancer cell death.

In summary, we studied the structural requirements for potent anticancer activity and substituents preferred for TOP1 inhibitory activity resulting in discovery of compounds **14h, p** with novel scaffold able to exhibit good anticancer effect and moderate TOP1 poisoning activity. Therefore, **14h** and **14p** can be considered as TOP1 inhibitors lead compounds will be optimized in our future study to attain more potential TOP1 inhibitors with potent anticancer activity.

2.5. Prediction of physicochemical and pharmacokinetic properties

SwissADME online web tool developed by the molecular modeling group of Swiss Institute of Bioinformatics (SIB) has been used to compute the physicochemical properties and predict the

druglikeness and pharmacokinetic properties of the most potent 4-alkoxy-2-arylquinolines **14e-h** and **14m-p** to verify that they are promising candidates from the aspect of pharmacokinetics [57].

The submitted compounds **14e-h** and **14m-p**, except **14o**, were predicted to display suitable physicochemical and pharmacokinetic properties; logP_{o/w} range 4.2–5.29, moderate water solubility, high GI absorption. Despite, compound **14o** had potent *in vitro* anticancer activity, it was predicted to have poor pharmacokinetic properties; logP_{o/w} 5.56, poor water solubility and low GI absorption. While, the chloro analogs **14e-h** were predicted to cross the blood brain barrier (BBB), the CF₃ analogs **14m-p** were not permeable to BBB, so no predicted CNS side effects (see supplementary data for more details) [58].

For high GI absorption and good oral bioavailability for a compound, the physicochemical properties should be in suitable ranges. The radar charts in Fig. 9 displayed the oral bioavailability of compounds **14h** and **14p** as representatives for the compounds in these series. This chart has six axes for the six parameters required for oral bioavailability; lipophilicity (LIPO), size (SIZE), polarity (POLAR), solubility (INSOLU), saturation (INSATU) and flexibility (FLEX) and the pink area in this plot represents the optimal ranges for predicted good oral bioavailability [59,60]. In Fig. 9, the red lines which represent compounds **14h** and **14p** are fully incorporated in the pink area predicting good oral bioavailability (see supplementary data for the radar charts of the remaining compounds). Moreover, SwissADME revealed that all tested compounds fulfilled Lipinski's rule as one of the major druglikeness characteristics developed by Pfizer pharmaceutical company predicting that these compounds with promising pharmacokinetic properties (see supplementary data) [61].

3. Conclusion

In summary, novel two series of 4-alkoxy-2-arylquinolines **14a-p** and **19a-c** were designed and synthesized as anticancer agents targeting TOP1 enzyme. The anticancer potential of all compounds have been evaluated according to the protocol of NCI. Based on these results, compound **14m** was the most potent with full panel GI₅₀ MG-MID 1.26 μ M affecting colon cancer, leukemia and melanoma at sub-micromolar level. Interestingly, compounds **14e-h** and **14m-p** showed good anticancer activity against nine cell lines of

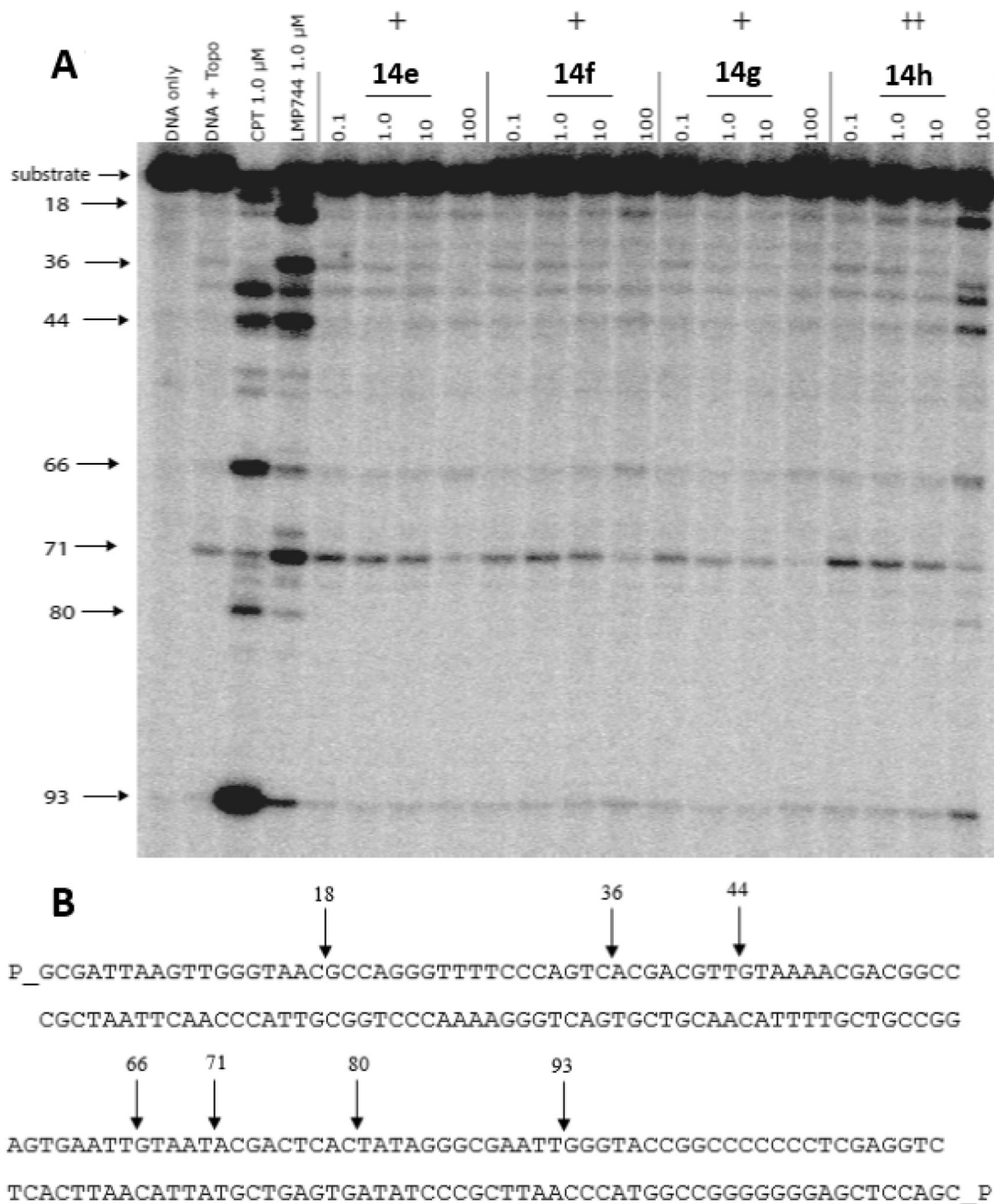


Fig. 7. (A) TOP1-mediated DNA cleavage induced by compounds **14e-h**. From the left: lane 1, DNA only; lane 2, DNA + TOP1; lane 3, CPT (1 μ M); lane 4, LMP744 (1 μ M); lanes 5–20, compounds **14e-h** at 0.1, 1, 10, 100 μ M. Arrows and numbers on the left represent the cleavage sites. (B) 3'-[32 P]-labeled 117-bp DNA oligonucleotide sequence with the positions of TOP1 cleavage sites.

different cancers at sub-micromolar concentration. Then, compound-induced TOP1-mediated DNA cleavage has been assayed for the promising compounds **14e-h** and **14m-p** to explore their ability to stabilize TOP1ccs. This study revealed that compounds **14h** and **14p** moderately stabilized TOP1ccs compared to 1 μ M CPT as the first 4-alkoxy-2-arylquinolines able to inhibit TOP1. Hence, compounds **14h** and **14p** were considered as lead compounds which can be optimized to develop more potent anticancer agents with potential TOP1 inhibitory activity. Finally, SwissADME online web tool predicted that compounds **14h** and **14p** possessed promising pharmacokinetics and druglikeness properties.

4. Experimental

4.1. Chemistry

4.1.1. General

Melting points were determined using Yanaco melting point device and were uncorrected. Infrared (IR) spectra were recorded by Jasco FT/IR-6600 spectrophotometer as KBr disks and were expressed in wavenumber (cm^{-1}). NMR spectra were measured using Bruker Advance III HD at 400 MHz for ^1H NMR, 100 MHz for ^{13}C NMR and 376 MHz for ^{19}F NMR in deuterated CDCl_3 , $\text{DMSO}-d_6$ or $\text{MeOH}-d_4$ using tetramethyl silane (TMS) as an internal standard.

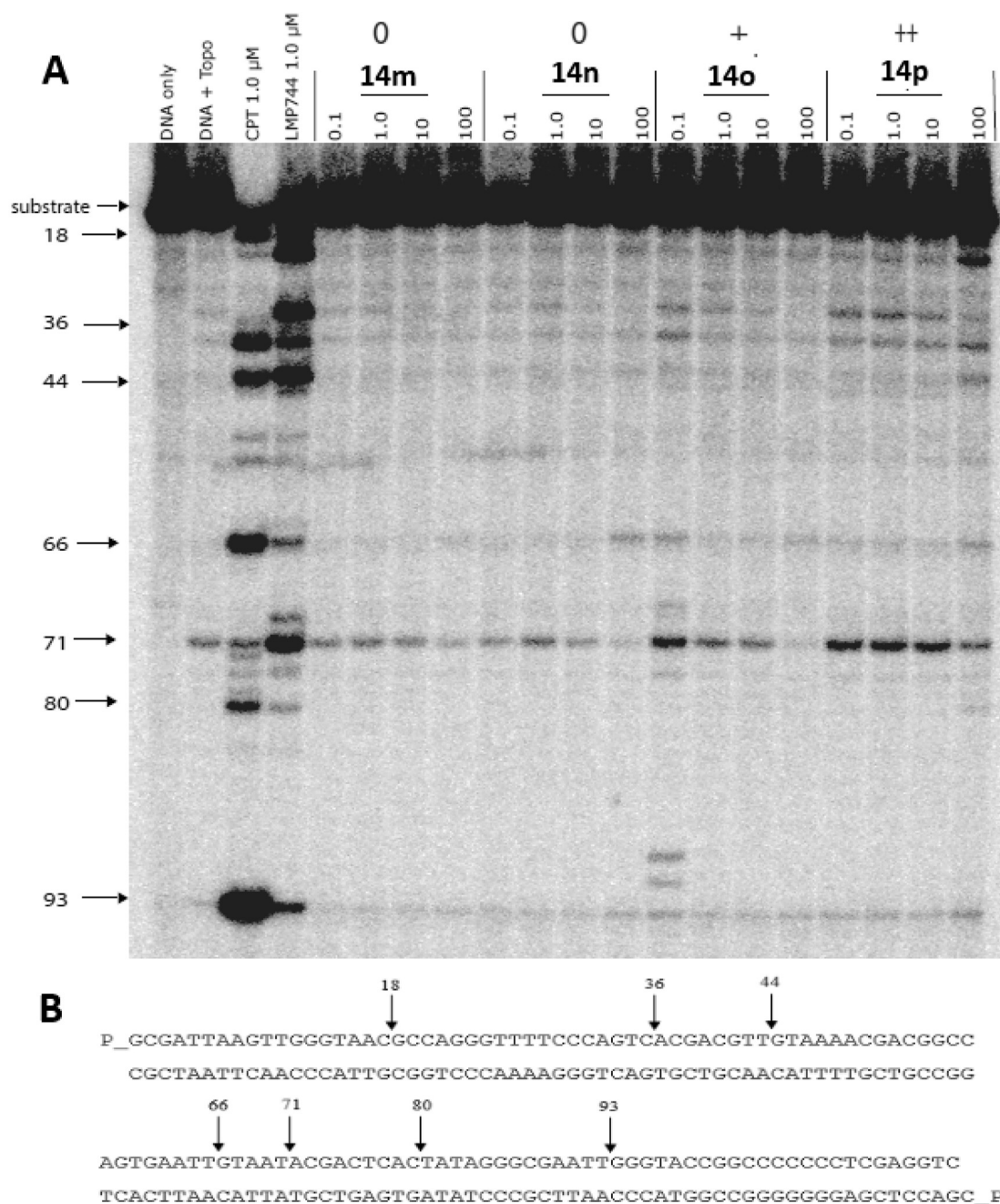


Fig. 8. (A) TOP1-mediated DNA cleavage induced by compounds **14m-p**. From the left: lane 1, DNA only; lane 2, DNA + TOP1; lane 3, CPT (1 μ M); lane 4, LMP744 (1 μ M); lanes 5–20, compounds **14m-p** at 0.1, 1, 10, 100 μ M. Arrows and numbers on the left represent the cleavage sites. (B) 3'-[32 P]-labeled 117-bp DNA oligonucleotide sequence with the positions of TOP1 cleavage sites.

Coupling constant values (J) were determined in Hertz (Hz) and chemical shifts (δ) were expressed in ppm. High resolution mass spectra (HRMS) were measured with Thermo Fisher Scientific LTQ Orbitrap XL spectrophotometer using electrospray ionization (ESI) and were expressed as $[M+H]^+$ or $[M+Na]^+$ at Natural Science Research and Development Center, Hiroshima University, Japan. The reaction mixtures were monitored by thin layer chromatography (TLC) using Merck silica gel 60F₂₅₄ aluminum sheets. Column chromatography was conducted using silica gel 60 N, 63–210 μ m that was purchased from Kanto Chemical Co. Inc. Unless otherwise mentioned, all solvents and chemical reagents were commercially available and were used without further purification.

4.1.2. Synthesis of 1-(2-amino-4,5-dimethoxyphenyl)ethenone (9)

The 2-aminoacetophenone derivative **9** was synthesized according to the reported experimental procedure [62,63].

Yellow solid, yield 70%, m.p. 100–102 $^{\circ}$ C; 1 H NMR (400 MHz, CDCl₃) δ (ppm): 2.53 (s, 3H, CH₃), 3.85 (s, 3H, OCH₃), 3.89 (s, 3H, OCH₃), 6.12 (s, 1H, phenyl CH), 6.27 (br s, 2H, NH₂), 7.12 (s, 1H, phenyl CH).

4.1.3. General procedure for synthesis of the benzoyl derivatives (11a, b)

Compound **9** (0.976 g, 5 mmol) was dissolved in dry THF (8 mL) and Et₃N (2 mL) and the mixture was cooled in ice bath. Then, a

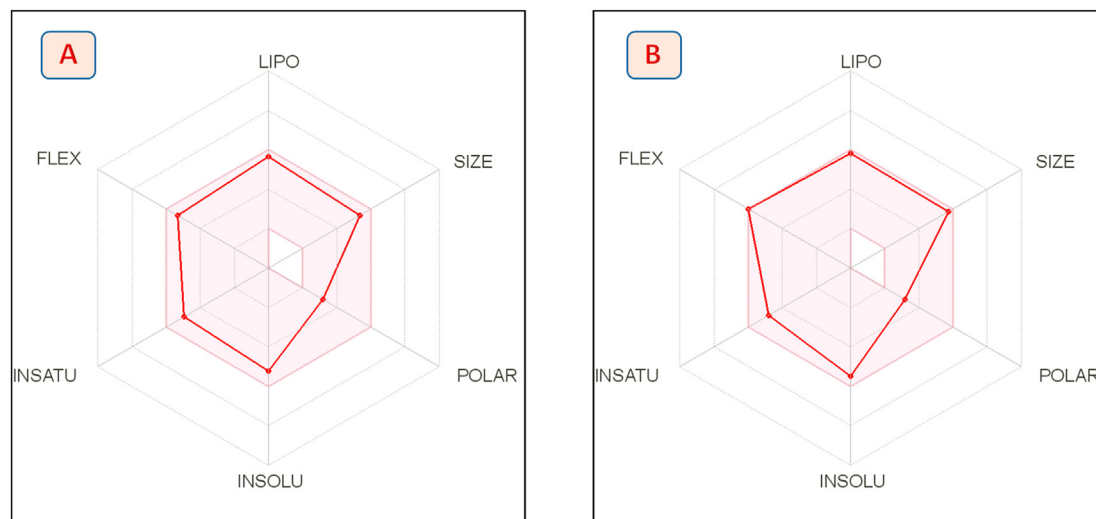


Fig. 9. Radar charts for prediction of oral bioavailability generated by SwissADME web tool; the pink area represents the ideal values for oral bioavailability and the red lines represent compounds (A) **14h** and (B) **14p**.

solution of the appropriate benzoyl chloride **10a, b** (5.1 mmol) in dry THF (2 mL) was added dropwise. After 30 min at 0 °C, the reaction mixture was stirred overnight at room temperature. After reaction completion, the reaction mixture was poured into ice water (50 mL). The precipitate separated was filtered off, washed several times with water then methanol, dried under vacuum and crystallized from acetone to afford compounds **11a, b** as yellow crystals.

4.1.3.1. N-(2-Acetyl-4,5-dimethoxyphenyl)-4-chlorobenzamide (11a). Yellow solid, yield 81%, m.p. 182–184 °C; IR (KBr, ν cm^{-1}): 3163 ($\text{NH}-\text{C}=\text{O}$), 3084, 3058 (CH aromatic), 2995, 2966, 2953, 2934 (CH aliphatic), 1720 ($\text{CH}_3\text{C}=\text{O}$), 1667 ($\text{NH}-\text{C}=\text{O}$), 1595 (C=C aromatic); ^1H NMR (400 MHz, CDCl_3) δ (ppm): 2.66 (s, 3H, CH_3), 3.92 (s, 3H, OCH_3), 4.02 (s, 3H, OCH_3), 7.31 (s, 1H, phenyl CH), 7.48 (d, 2H, benzoyl 2CH, $J = 8.6$ Hz), 7.99 (d, 2H, benzoyl 2CH, $J = 8.6$ Hz), 8.71 (s, 1H, phenyl CH), 13.01 (s, 1H, NH); ^{13}C NMR (100 MHz, CDCl_3) δ (ppm): 28.50, 56.37, 56.49, 103.56, 113.89, 114.64, 128.95, 129.17, 133.28, 138.21, 138.40, 143.91, 155, 165.07 (C=O), 201.35 (C=O); HRESIMS (m/z): $[\text{M}+\text{Na}]^+$ Calcd for $\text{C}_{17}\text{H}_{16}\text{ClNO}_4\text{Na}$, 356.06601; found, 356.06613.

4.1.3.2. N-(2-Acetyl-4,5-dimethoxyphenyl)-4-(trifluoromethyl)benzamide (11b). Yellow solid, Yield 85%, m.p. 128–130 °C; IR (KBr, ν cm^{-1}): 3160 ($\text{NH}-\text{C}=\text{O}$), 3061, 3002 (CH aromatic), 2973, 2950, 2934, 2908 (CH aliphatic), 1740 ($\text{CH}_3\text{C}=\text{O}$), 1640 ($\text{NH}-\text{C}=\text{O}$), 1598 (C=C aromatic); ^1H NMR (400 MHz, CDCl_3) δ (ppm): 2.63 (s, 3H, CH_3), 3.89 (s, 3H, OCH_3), 4 (s, 3H, OCH_3), 7.27 (s, 1H, phenyl CH), 7.75 (d, 2H, benzoyl 2CH, $J = 8.2$ Hz), 8.13 (d, 2H, benzoyl 2CH, $J = 8.2$ Hz), 8.67 (s, 1H, phenyl CH), 13.07 (s, 1H, NH); ^{13}C NMR (100 MHz, CDCl_3) δ (ppm): 28.33, 56.24, 56.31, 103.47, 113.73, 114.60, 123.69 (CF_3 , q, $J = 272.6$ Hz), 125.80 ($\text{CH}-\text{C}-\text{CF}_3$, q, $J = 3.6$ Hz), 127.83, 133.49 ($\text{CH}-\text{C}-\text{CF}_3$, q, $J = 32.7$ Hz), 137.80, 138.01, 143.95, 154.85, 164.57 (C=O), 201.31 (C=O); ^{19}F NMR (376.46 MHz, CDCl_3) δ (ppm): 62.98 (s); HRESIMS (m/z): $[\text{M}+\text{Na}]^+$ Calcd for $\text{C}_{18}\text{H}_{16}\text{F}_3\text{NO}_4\text{Na}$, 390.09236; found, 390.09268.

4.1.4. General procedures for synthesis of the quinolones (12a, b)

A mixture of **11a** or **11b** (1 equivalent), sodium hydroxide (3 equivalents) in dry dioxane was refluxed under N_2 at 110 °C for 4 h, then removed from oil bath and allowed to cool to room

temperature. Small amount of water and large amount of hexane were added to the reaction mixture, then the flask was sonicated for 2 min. The biphasic mixture was neutralized to pH 7 with 1 M HCl. The separated solid was filtered, washed with water and dried to afford **12a** or **b**, respectively.

4.1.4.1. 2-(4-Chlorophenyl)-6,7-dimethoxyquinolin-4(1H)-one (12a). Yellow solid, Yield 91%, m.p. > 250 °C; IR (KBr, ν cm^{-1}): 3400 (NH), 3088 (CH aromatic), 2963, 2940 (CH aliphatic), 1685 (C=O), 1507, 1466 (C=C aromatic); ^1H NMR (400 MHz, $\text{MeOH}-d_4$) δ (ppm): 4.03 (s, 3H, OCH_3), 4.06 (s, 3H, OCH_3), 7.02 (s, 1H, vinyl CH), 7.41 (s, 1H, phenyl CH), 7.62 (s, 1H, phenyl CH), 7.64 (d, 2H, chlorophenyl 2CH, $J = 8.6$ Hz), 7.84 (d, 2H, chlorophenyl 2CH, $J = 8.6$ Hz); ^{13}C NMR (100 MHz, $\text{MeOH}-d_4$) δ (ppm): 55.78, 56.02, 99.02, 102.21, 104.43, 116.35, 128.40, 128.99, 129.53, 131.02, 131.35, 137.33, 137.72, 149.65, 150.47, 155.93, 171.88 (C=O); HRESIMS (m/z): $[\text{M}+\text{H}]^+$ Calcd for $\text{C}_{17}\text{H}_{15}\text{ClNO}_3$, 316.07350; found, 316.07397.

4.1.4.2. 6,7-Dimethoxy-2-(4-(trifluoromethyl)phenyl)quinolin-4(1H)-one (12b). Yellow solid, Yield 90%, m.p. > 250 °C; IR (KBr, ν cm^{-1}): 3266 (NH), 3090 (CH aromatic), 2960 (CH aliphatic), 1685 (C=O), 1581, 1518 (C=C aromatic); ^1H NMR (400 MHz, $\text{DMSO}-d_6$) δ (ppm): 3.90 (s, 3H, OCH_3), 3.93 (s, 3H, OCH_3), 6.83 (s, 1H, vinyl CH), 7.44 (s, 1H, phenyl CH), 7.49 (s, 1H, phenyl CH), 7.98 (d, 2H, CF_3 -phenyl 2CH, $J = 8.3$ Hz), 8.11 (d, 2H, CF_3 -phenyl 2CH, $J = 8.3$ Hz); ^{13}C NMR (100 MHz, $\text{MeOH}-d_4$) δ (ppm): 56.27, 56.51, 100.86, 102.78, 105.62, 117.13, 124.38 (CF_3 , q, $J = 272.4$ Hz), 126.45 ($\text{CH}-\text{C}-\text{CF}_3$, q, $J = 3.8$ Hz), 129.10, 131.16 ($\text{CH}-\text{C}-\text{CF}_3$, q, $J = 32.1$ Hz), 137.86, 148.93, 149.21, 154.82, 171.58 (C=O); ^{19}F NMR (376.46 MHz, CDCl_3) δ (ppm): 61.28 (s); HRESIMS (m/z): $[\text{M}+\text{H}]^+$ Calcd for $\text{C}_{18}\text{H}_{15}\text{F}_3\text{NO}_3$, 350.10058; found, 350.09995.

4.1.5. General procedure for synthesis of the key intermediates (13a-d)

A mixture of **12a** or **b** (3 mmol), KOH (1.009 g, 18 mmol) and KI (0.498 g, 3 mmol) was stirred in dry DMF (30 mL) for 2 h, then the respective 1-bromo-2-chloroethane or 1-bromo-3-chloropropane (15 mmol) was added. The reaction mixture was stirred for 24 h at room temperature. After completion of the reaction, reaction mixture was poured into ice water (50 mL) and the precipitated solid was filtered off, washed with water then hexane and

dried to afford compounds **13a-d** that were used without further purification.

4.1.5.1. 4-(2-Chloroethoxy)-2-(4-chlorophenyl)-6,7-dimethoxyquinoline (13a). White solid, Yield 89%, m.p. 170–172 °C; IR (KBr, ν cm⁻¹): 3090, 3016 (CH aromatic), 2990, 2967, 2945, 2887 (CH aliphatic), 1596, 1582, 1560, 1512 (C=C aromatic); ¹H NMR (400 MHz, CDCl₃) δ (ppm): 3.98 (t, 2H, CH₂Cl, *J* = 5.8 Hz), 4.02 (s, 3H, OCH₃), 4.03 (s, 3H, OCH₃), 4.49 (t, 2H, CH₂-O, *J* = 5.8 Hz), 6.98 (s, 1H, vinyl CH), 7.40 (s, 1H, phenyl CH), 7.41 (s, 1H, phenyl CH), 7.44 (d, 2H, chlorophenyl 2CH, *J* = 8.6 Hz), 7.98 (d, 2H, chlorophenyl 2CH, *J* = 8.6 Hz); ¹³C NMR (100 MHz, CDCl₃) δ (ppm): 41.54, 56.10, 56.13, 68.08, 97.34, 99.62, 108.18, 114.78, 128.49, 128.87, 135.04, 138.70, 146.32, 149.29, 152.93, 155.37, 160.30; HRESIMS (*m/z*): [M+H]⁺ Calcd for C₁₉H₁₈Cl₂NO₃, 378.06655; found, 378.06598.

4.1.5.2. 2-(4-Chlorophenyl)-4-(3-chloropropoxy)-6,7-dimethoxyquinoline (13b). White solid, Yield 83%, m.p. 143.145 °C; IR (KBr, ν cm⁻¹): 3079, 3061, 3000 (CH aromatic), 2960, 2936, 2875 (CH aliphatic), 1592, 1559, 1513 (C=C aromatic); ¹H NMR (400 MHz, CDCl₃) δ (ppm): 2.43 (p, 2H, CH₂, *J* = 6.1 Hz) 3.83 (t, 2H, CH₂Cl, *J* = 6.2 Hz), 4.02 (s, 3H, OCH₃), 4.03 (s, 3H, OCH₃), 4.42 (t, 2H, CH₂-O, *J* = 6 Hz), 7.06 (s, 1H, vinyl CH), 7.35 (s, 1H, phenyl CH), 7.42 (s, 1H, phenyl CH), 7.45 (d, 2H, chlorophenyl 2CH, *J* = 8.6 Hz), 8 (d, 2H, chlorophenyl 2CH, *J* = 8.6 Hz); ¹³C NMR (100 MHz, CDCl₃) δ (ppm): 31.97, 41.35, 56.07, 56.13, 64.90, 97.37, 99.54, 108.29, 114.81, 128.53, 128.85, 134.98, 138.84, 146.24, 149.17, 152.81, 155.54, 160.74; HRESIMS (*m/z*): [M+H]⁺ Calcd for C₂₀H₂₀Cl₂NO₃, 392.08148; found, 392.08127.

4.1.5.3. 4-(2-Chloroethoxy)-6,7-dimethoxy-2-(4-(trifluoromethyl)phenyl)quinoline (13c). White solid, Yield 81%, m.p. 158–160 °C; IR (KBr, ν cm⁻¹): 3095, 3061, 3015 (CH aromatic), 2958, 2943, 2909, 2887 (CH aliphatic), 1587, 1565, 1509 (C=C aromatic); ¹H NMR (400 MHz, CDCl₃) δ (ppm): 4 (t, 2H, CH₂Cl, *J* = 5.8 Hz), 4.04 (s, 3H, OCH₃), 4.05 (s, 3H, OCH₃), 4.52 (t, 2H, CH₂-O, *J* = 5.8 Hz), 7.05 (s, 1H, vinyl CH), 7.43 (s, 1H, phenyl CH), 7.44 (s, 1H, phenyl CH), 7.73 (d, 2H, CF₃-phenyl 2CH, *J* = 8.2 Hz), 8.15 (d, 2H, CF₃-phenyl 2CH, *J* = 8.2 Hz); ¹³C NMR (100 MHz, CDCl₃) δ (ppm): 41.51, 56.11, 56.15, 68.16, 97.66, 99.60, 108.27, 115.05, 124.23 (CF₃, q, *J* = 272.1 Hz), 125.63 (CH-C-CF₃, q, *J* = 3.7 Hz), 127.52, 130.72 (CH-C-CF₃, q, *J* = 32.5 Hz), 143.64, 146.40, 149.57, 153.08, 155.02, 160.40; ¹⁹F NMR (376.46 MHz, CDCl₃) δ (ppm): 62.49 (s); HRESIMS (*m/z*): [M+H]⁺ Calcd for C₂₀H₁₈ClF₃NO₃, 412.09218; found, 412.09201.

4.1.5.4. 4-(3-Chloropropoxy)-6,7-dimethoxy-2-(4-(trifluoromethyl)phenyl)quinoline (13d). White solid, Yield 78%, m.p. 133–135 °C; IR (KBr, ν cm⁻¹): 3079, 3015 (CH aromatic), 2961, 2934, 2912, 2883 (CH aliphatic), 1592, 1564, 1507 (C=C aromatic); ¹H NMR (400 MHz, CDCl₃) δ (ppm): 2.45 (p, 2H, CH₂, *J* = 6.1 Hz), 43.84 (t, 2H, CH₂Cl, *J* = 6.2 Hz), 4.03 (s, 3H, OCH₃), 4.04 (s, 3H, OCH₃), 4.45 (t, 2H, CH₂-O, *J* = 6 Hz), 7.12 (s, 1H, vinyl CH), 7.38 (s, 1H, phenyl CH), 7.45 (s, 1H, phenyl CH), 7.74 (d, 2H, CF₃-phenyl 2CH, *J* = 8.1 Hz), 8.17 (d, 2H, CF₃-phenyl 2CH, *J* = 8.1 Hz); ¹³C NMR (100 MHz, CDCl₃) δ (ppm): 31.95, 41.31, 56.09, 56.14, 64.98, 97.69, 99.51, 108.36, 115.07, 124.25 (CF₃, q, *J* = 271.9 Hz), 125.61 (CH-C-CF₃, q, *J* = 3.7 Hz), 127.56, 130.67 (CH-C-CF₃, q, *J* = 32.4 Hz), 143.78, 146.32, 149.45, 152.95, 155.20, 160.84; ¹⁹F NMR (376.46 MHz, CDCl₃) δ (ppm): 62.48 (s); HRESIMS (*m/z*): [M+H]⁺ Calcd for C₂₁H₂₀ClF₃NO₃, 426.10783; found, 426.10803.

4.1.6. General procedure for synthesis of the target 4-alkoxy-2-arylquinolines (14a-p)

A mixture of **13a-d** (1 mmol), KI (0.83 g, 5 mmol) and anhydrous K₂CO₃ (1.38 g, 10 mmol) was stirred in dry DMF (20 mL) for 30 min.

Then, the appropriate amine (10 mmol) was added to the mixture. The reaction mixture was refluxed at 90 °C for 12 h, then poured into ice water (50 mL). The precipitated solid was filtered off, washed with water then hexane, dried and purified by silica gel column chromatography using DCM/MeOH affording **14a-p** in pure form.

4.1.6.1. 2-(4-Chlorophenyl)-6,7-dimethoxy-4-(2-(pyrrolidin-1-yl)ethoxy)quinoline (14a). White solid, Yield 80%, m.p. 110–112 °C; IR (KBr, ν cm⁻¹): 3000 (CH aromatic), 2961, 2936, 2872 (CH aliphatic), 1592, 1559, 1513 (C=C aromatic); ¹H NMR (400 MHz, CDCl₃) δ (ppm): 1.85 (p, 4H, pyrrolidinyl 2CH₂, *J* = 3.3 Hz), 2.75 (s, 4H, pyrrolidinyl 2CH₂-N), 3.12 (t, 2H, CH₂-N, *J* = 6 Hz), 4.02 (s, 3H, OCH₃), 4.04 (s, 3H, OCH₃), 4.43 (t, 2H, CH₂-O, *J* = 6 Hz), 7.07 (s, 1H, vinyl CH), 7.42 (s, 2H, phenyl CH), 7.46 (d, 2H, chlorophenyl 2CH, *J* = 8.6 Hz), 8 (d, 2H, chlorophenyl 2CH, *J* = 8.6 Hz); ¹³C NMR (100 MHz, CDCl₃) δ (ppm): 23.60, 54.59, 54.98, 56.02, 56.12, 67.77, 97.44, 99.86, 108.21, 114.94, 128.54, 128.86, 134.95, 138.94, 146.23, 149.07, 152.75, 155.63, 160.93; HRESIMS (*m/z*): [M+H]⁺ Calcd for C₂₃H₂₆ClN₂O₃, 413.16337; found, 413.16309.

4.1.6.2. 1-(2-((2-(4-Chlorophenyl)-6,7-dimethoxyquinolin-4-yl)oxy)ethyl)piperidin-4-ol (14b). White solid, Yield 72%, m.p. 205–207 °C; IR (KBr, ν cm⁻¹): 3226 (OH), 3000 (CH aromatic), 2936, 2918 (CH aliphatic), 1592, 1560 (C=C aromatic); ¹H NMR (400 MHz, CDCl₃) δ (ppm): 1.59–1.68 (m, 3H, piperidinyl 2CHH' and OH), 1.90–1.96 (m, 2H, piperidinyl 2CHH'), 2.38–2.44 (m, 2H, piperidinyl 2CHH'-N), 2.95 (p, 2H, piperidinyl 2CHH'-N, *J* = 5.3 Hz), 3.12 (t, 2H, CH₂-N, *J* = 6 Hz), 3.71–3.78 (m, 1H, piperidinyl CH-OH), 4.01 (s, 3H, OCH₃), 4.03 (s, 3H, OCH₃), 4.39 (t, 2H, CH₂-O, *J* = 6 Hz), 7.06 (s, 1H, vinyl CH), 7.38 (s, 1H, phenyl CH), 7.42 (s, 1H, phenyl CH), 7.45 (d, 2H, chlorophenyl 2CH, *J* = 8.6 Hz), 8 (d, 2H, chlorophenyl 2CH, *J* = 8.6 Hz); ¹³C NMR (100 MHz, CDCl₃) δ (ppm): 34.52, 51.63, 56.01, 56.13, 56.73, 66.87, 67.54, 97.45, 99.76, 108.23, 114.92, 128.53, 128.86, 134.97, 138.91, 146.22, 149.10, 152.77, 155.60, 160.90; HRESIMS (*m/z*): [M+H]⁺ Calcd for C₂₄H₂₈ClN₂O₄, 443.17321; found, 443.17334.

4.1.6.3. 2-(4-Chlorophenyl)-6,7-dimethoxy-4-(2-(piperidin-1-yl)ethoxy)quinoline (14c). White solid, Yield 87%, m.p. 142–144 °C; IR (KBr, ν cm⁻¹): 3089, 3006 (CH aromatic), 2952, 2928 (CH aliphatic), 1592, 1560, 1513 (C=C aromatic); ¹H NMR (400 MHz, CDCl₃) δ (ppm): 1.47 (p, 2H, piperidinyl CH₂, *J* = 6.1 Hz), 1.63 (p, 4H, piperidinyl 2CH₂, *J* = 5.5 Hz), 2.60 (t, 4H, piperidinyl 2CH₂-N, *J* = 4.8 Hz), 2.96 (t, 2H, CH₂-N, *J* = 6.1 Hz), 4.02 (s, 3H, OCH₃), 4.03 (s, 3H, OCH₃), 4.40 (t, 2H, CH₂-O, *J* = 6.1 Hz), 7.07 (s, 1H, vinyl CH), 7.40 (s, 1H, phenyl CH), 7.42 (s, 1H, phenyl CH), 7.45 (d, 2H, chlorophenyl 2CH, *J* = 8.6 Hz), 8 (d, 2H, chlorophenyl 2CH, *J* = 8.6 Hz); ¹³C NMR (100 MHz, CDCl₃) δ (ppm): 24.12, 26.10, 55.23, 56.00, 56.11, 57.60, 66.81, 97.47, 99.84, 108.22, 114.97, 128.53, 128.84, 134.93, 138.95, 146.21, 149.06, 152.74, 155.60, 165.98; HRESIMS (*m/z*): [M+H]⁺ Calcd for C₂₄H₂₈ClN₂O₃, 427.17830; found, 427.17825.

4.1.6.4. 4-(2-((2-(4-Chlorophenyl)-6,7-dimethoxyquinolin-4-yl)oxy)ethyl)morpholine (14d). White solid, Yield 88%, m.p. 131–133 °C; IR (KBr, ν cm⁻¹): 3094, 3055, 3019 (CH aromatic), 2950, 2923, 2879 (CH aliphatic), 1592, 1560, 1513 (C=C aromatic); ¹H NMR (400 MHz, CDCl₃) δ (ppm): 2.66 (t, 4H, morpholinyl CH₂-N, *J* = 4.6 Hz), 2.99 (t, 2H, CH₂-N, *J* = 5.8 Hz), 3.74 (t, 4H, morpholinyl 2CH₂-O, *J* = 4.6 Hz), 4.01 (s, 3H, OCH₃), 4.03 (s, 3H, OCH₃), 4.40 (t, 2H, CH₂-O, *J* = 5.8 Hz), 7.04 (s, 1H, vinyl CH), 7.37 (s, 1H, phenyl CH), 7.41 (s, 1H, phenyl CH), 7.45 (d, 2H, chlorophenyl 2CH, *J* = 8.6 Hz), 7.99 (d, 2H, chlorophenyl 2CH, *J* = 8.6 Hz); ¹³C NMR (100 MHz, CDCl₃) δ (ppm): 54.21, 55.99, 56.13, 57.33, 66.57, 67.01, 97.39, 99.68, 108.25, 114.88, 128.51, 128.86, 134.98, 138.88, 146.22, 149.13, 152.79, 155.55, 160.81;

HRESIMS (m/z): $[M+H]^+$ Calcd for $C_{23}H_{26}ClN_2O_4$, 429.15756; found, 429.15778.

4.1.6.5. 2-(4-Chlorophenyl)-6,7-dimethoxy-4-(3-(pyrrolidin-1-yl)propoxy)quinoline (**14e**). White solid, Yield 92%, m.p. 116–118 °C; IR (KBr, ν cm^{-1}): 3090, 3061, 3000 (CH aromatic), 2955, 2905, 2876 (CH aliphatic), 1591, 1560, 1512 (C=C aromatic); 1H NMR (400 MHz, $CDCl_3$) δ (ppm): 1.81 (p, 4H, pyrrolidinyl $2CH_2$, $J = 3.3$ Hz), 2.2 (p 2H, CH_2 , $J = 6.8$ Hz), 2.56 (s, 4H, pyrrolidinyl $2CH_2-N$), 2.72 (t, 2H, CH_2-N , $J = 7.3$ Hz), 4.02 (s, 3H, OCH_3), 4.03 (s, 3H, OCH_3), 4.34 (t, 2H, CH_2-O , $J = 6.4$ Hz), 7.07 (s, 1H, vinyl CH), 7.40 (s, 1H, phenyl CH), 7.41 (s, 1H, phenyl CH) 7.45 (d, 2H, chlorophenyl $2CH$, $J = 8.5$ Hz), 8 (d, 2H, chlorophenyl $2CH$, $J = 8.5$ Hz); ^{13}C NMR (100 MHz, $CDCl_3$) δ (ppm): 23.49, 28.70, 53.12, 54.34, 56.06, 56.11, 66.83, 97.44, 99.76, 108.23, 114.97, 128.55, 128.81, 134.88, 139.00, 146.18, 149.04, 152.71, 155.61, 161.15; HRESIMS (m/z): $[M+H]^+$ Calcd for $C_{24}H_{28}ClN_2O_3$, 427.17830; found, 427.17853.

4.1.6.6. 1-(3-((2-(4-Chlorophenyl)-6,7-dimethoxyquinolin-4-yl)oxy)propyl)piperidin-4-ol (**14f**). White solid, Yield 76%, m.p. 155–157 °C; IR (KBr, ν cm^{-1}): 3410 (OH), 3009 (CH aromatic), 2924 (CH aliphatic), 1589, 1560, 1513 (C=C aromatic); 1H NMR (400 MHz, $CDCl_3$) δ (ppm): 1.56–1.64 (m, 3H, piperidinyl $2CHH'$), 1.68 (br s, 1H, OH), 1.89–1.93 (m, 2H, piperidinyl $2CHH'$), 2.12–2.22 (m, 4H, piperidinyl $2CHH'-N$, CH_2), 2.60 (t, 2H, CH_2-N , $J = 7.3$ Hz), 2.82 (t, 2H, piperidinyl $2CHH'-N$, $J = 5.7$ Hz), 3.70–3.75 (m, 1H, piperidinyl $CH-OH$), 4.02 (s, 3H, OCH_3), 4.03 (s, 3H, OCH_3), 4.31 (t, 2H, CH_2-O , $J = 6.4$ Hz), 7.04 (s, 1H, vinyl CH), 7.39 (s, 1H, phenyl CH), 7.42 (s, 1H, phenyl CH), 7.45 (d, 2H, chlorophenyl $2CH$, $J = 8.6$ Hz), 8 (d, 2H, chlorophenyl $2CH$, $J = 8.6$ Hz); ^{13}C NMR (100 MHz, $CDCl_3$) δ (ppm): 26.91, 34.48, 51.20, 55.01, 56.06, 56.11, 66.74, 67.87, 97.41, 99.72, 108.24, 114.95, 128.56, 128.82, 134.92, 139.00, 146.20, 149.08, 152.75, 155.63, 161.11; HRESIMS (m/z): $[M+H]^+$ Calcd for $C_{25}H_{30}ClN_2O_4$, 457.18886; found, 457.18893.

4.1.6.7. 2-(4-Chlorophenyl)-6,7-dimethoxy-4-(3-(piperidin-1-yl)propoxy)quinoline (**14g**). White solid, Yield 76%, m.p. 130.132 °C; IR (KBr, ν cm^{-1}): 3095, 3000 (CH aromatic), 2930, 2880 (CH aliphatic), 1591, 1560, 1512 (C=C aromatic); 1H NMR (400 MHz, $CDCl_3$) δ (ppm): 1.45 (t, 2H, piperidinyl CH_2 , $J = 5.6$ Hz), 1.60 (p, 4H, piperidinyl $2CH_2$, $J = 5.6$ Hz), 2.15 (p, 2H, CH_2 , $J = 6.9$ Hz), 2.43 (br s, 4H, piperidinyl $2CH_2-N$), 2.56 (t, 2H, CH_2-N , $J = 7.4$ Hz), 4.01 (s, 3H, OCH_3), 4.02 (s, 3H, OCH_3), 4.29 (t, 2H, CH_2-O , $J = 6.4$ Hz), 7.03 (s, 1H, vinyl CH), 7.38 (s, 1H, phenyl CH), 7.40 (s, 1H, phenyl CH), 7.44 (d, 2H, chlorophenyl $2CH$, $J = 8.6$ Hz), 7.99 (d, 2H, chlorophenyl $2CH$, $J = 8.6$ Hz); ^{13}C NMR (100 MHz, $CDCl_3$) δ (ppm): 24.41, 25.99, 26.68, 54.76, 55.95, 56.04, 56.09, 66.92, 97.39, 99.76, 108.21, 114.98, 128.55, 128.80, 134.88, 139.00, 146.17, 149.04, 152.71, 155.59, 161.13; HRESIMS (m/z): $[M+H]^+$ Calcd for $C_{25}H_{30}ClN_2O_3$, 441.19395; found, 441.19409.

4.1.6.8. 4-(3-((2-(4-Chlorophenyl)-6,7-dimethoxyquinolin-4-yl)oxy)propyl)morpholine (**14h**). White solid, Yield 79%, m.p. 144–146 °C; IR (KBr, ν cm^{-1}): 3091, 3064, 3027, 3004 (CH aromatic), 2951, 2903, 2883 (CH aliphatic), 1590, 1559, 1511 (C=C aromatic); 1H NMR (400 MHz, $CDCl_3$) δ (ppm): 2.16 (p, 2H, CH_2 , $J = 6.8$ Hz), 2.50 (t, 4H, morpholinyl CH_2-N , $J = 4.4$ Hz), 2.61 (t, 2H, CH_2-N , $J = 7.2$ Hz), 3.72 (t, 4H, morpholinyl $2CH_2-O$, $J = 4.4$ Hz), 4.02 (s, 3H, OCH_3), 4.03 (s, 3H, OCH_3), 4.33 (t, 2H, CH_2-O , $J = 6.4$ Hz), 7.04 (s, 1H, vinyl CH), 7.38 (s, 1H, phenyl CH), 7.41 (s, 1H, phenyl CH), 7.45 (d, 2H, chlorophenyl $2CH$, $J = 8.6$ Hz), 8 (d, 2H, chlorophenyl $2CH$, $J = 8.6$ Hz); ^{13}C NMR (100 MHz, $CDCl_3$) δ (ppm): 26.26, 53.84, 55.51, 56.05, 56.11, 66.51, 66.97, 97.37, 99.68, 108.27, 114.92, 128.54, 128.83, 134.93, 138.99, 146.21, 149.10, 152.76, 155.60, 161.07; HRESIMS (m/z): $[M+H]^+$ Calcd for $C_{24}H_{28}ClN_2O_4$, 443.17321; found, 443.17340.

4.1.6.9. 6,7-Dimethoxy-4-(2-(pyrrolidin-1-yl)ethoxy)-2-(4-(trifluoromethyl)phenyl)quinoline (**14i**). White solid, Yield 86%, m.p. 116–118 °C; IR (KBr, ν cm^{-1}): 3096, 3019 (CH aromatic), 2954, 2878 (CH aliphatic), 1592, 1560, 1522, 1509 (C=C aromatic); 1H NMR (400 MHz, $CDCl_3$) δ (ppm): 1.83 (p, 4H, pyrrolidinyl $2CH_2$, $J = 3.4$ Hz), 2.73 (p, 4H, pyrrolidinyl $2CH_2-N$, $J = 3.4$ Hz), 3.10 (t, 2H, CH_2-N , $J = 6$ Hz), 4.02 (s, 3H, OCH_3), 4.04 (s, 3H, OCH_3), 4.43 (t, 2H, CH_2-O , $J = 6$ Hz), 7.10 (s, 1H, vinyl CH), 7.43 (s, 1H, phenyl CH), 7.44 (s, 1H, phenyl CH), 7.73 (d, 2H, CF_3 -phenyl $2CH$, $J = 8.1$ Hz), 8.16 (d, 2H, CF_3 -phenyl $2CH$, $J = 8.1$ Hz); ^{13}C NMR (100 MHz, $CDCl_3$) δ (ppm): 23.62, 54.62, 55.00, 56.02, 56.12, 67.99, 97.71, 99.85, 108.28, 115.21, 124.25 (CF_3 , q, $J = 272$ Hz), 125.60 ($CH-C-CF_3$, q, $J = 3.7$ Hz), 127.55, 130.62 ($CH-C-CF_3$, q, $J = 32$ Hz), 143.88, 146.28, 149.32, 152.87, 155.23, 161.06; ^{19}F NMR (376.46 MHz, $CDCl_3$) δ (ppm): 62.49 (s); HRESIMS (m/z): $[M+H]^+$ Calcd for $C_{24}H_{26}F_3N_2O_3$, 447.18900; found, 447.18820.

4.1.6.10. 1-(2-((6,7-Dimethoxy-2-(4-(trifluoromethyl)phenyl)quinolin-4-yl)oxy)ethyl)piperidin-4-ol (**14j**). White solid, Yield 76%, m.p. 176–178 °C; IR (KBr, ν cm^{-1}): 3360 (OH), 3006 (CH aromatic), 2945, 2925, 2900 (CH aliphatic), 1591, 1566, 1511 (C=C aromatic); 1H NMR (400 MHz, $CDCl_3$) δ (ppm): 1.59–1.67 (m, 2H, piperidinyl $2CHH'$), 1.84 (br s, 1H, OH), 1.89–1.94 (m, 2H, piperidinyl $2CHH'$), 2.38–2.44 (m, 2H, piperidinyl $2CHH'-N$), 2.95 (p, 2H, piperidinyl $2CHH'-N$, $J = 5.2$ Hz), 2.99 (t, 2H, CH_2-N , $J = 6$ Hz), 3.71–3.76 (m, 1H, piperidinyl $CH-OH$), 4.01 (s, 3H, OCH_3), 4.03 (s, 3H, OCH_3), 4.40 (t, 2H, CH_2-O , $J = 6$ Hz), 7.09 (s, 1H, vinyl CH), 7.39 (s, 1H, phenyl CH), 7.44 (s, 1H, phenyl CH), 7.73 (d, 2H, CF_3 -phenyl $2CH$, $J = 8.2$ Hz), 8.15 (d, 2H, CF_3 -phenyl $2CH$, $J = 8.2$ Hz); ^{13}C NMR (100 MHz, $CDCl_3$) δ (ppm): 34.41, 51.59, 56.02, 56.13, 56.69, 66.83, 67.38, 97.77, 99.73, 108.24, 115.16, 124.24 (CF_3 , q, $J = 272.1$ Hz), 125.60 ($CH-C-CF_3$, q, $J = 3.7$ Hz), 127.57, 130.65 ($CH-C-CF_3$, q, $J = 32.4$ Hz), 143.81, 146.26, 149.38, 152.91, 155.24, 160.97; ^{19}F NMR (376.46 MHz, $CDCl_3$) δ (ppm): 62.48 (s); HRESIMS (m/z): $[M+H]^+$ Calcd for $C_{25}H_{27}F_3N_2O_4$, 477.19957; found, 477.19897.

4.1.6.11. 6,7-Dimethoxy-4-(2-(piperidin-1-yl)ethoxy)-2-(4-(trifluoromethyl)phenyl)quinoline (**14k**). White solid, Yield 90%, m.p. 138–140 °C; IR (KBr, ν cm^{-1}): 3096, 3009 (CH aromatic), 2939 (CH aliphatic), 1592, 1560, 1508 (C=C aromatic); 1H NMR (400 MHz, $CDCl_3$) δ (ppm): 1.47 (p, 2H, piperidinyl CH_2 , $J = 5.4$ Hz), 1.63 (p, 4H, piperidinyl $2CH_2$, $J = 5.6$ Hz), 2.61 (t, 4H, piperidinyl $2CH_2-N$, $J = 5.8$ Hz), 2.97 (t, 2H, CH_2-N , $J = 6.1$ Hz), 4.03 (s, 3H, OCH_3), 4.04 (s, 3H, OCH_3), 4.42 (t, 2H, CH_2-O , $J = 6.1$ Hz), 7.12 (s, 1H, vinyl CH), 7.42 (s, 1H, phenyl CH), 7.44 (s, 1H, phenyl CH), 7.74 (d, 2H, CF_3 -phenyl $2CH$, $J = 8.2$ Hz), 8.17 (d, 2H, CF_3 -phenyl $2CH$, $J = 8.2$ Hz); ^{13}C NMR (100 MHz, $CDCl_3$) δ (ppm): 24.11, 26.08, 55.23, 56.01, 56.12, 57.59, 66.88, 97.77, 99.81, 108.28, 115.22, 124.26 (CF_3 , q, $J = 272$ Hz), 125.59 ($CH-C-CF_3$, q, $J = 3.7$ Hz), 127.54, 130.62 ($CH-C-CF_3$, q, $J = 32.4$ Hz), 143.87, 146.27, 149.33, 152.87, 155.21, 161.06; ^{19}F NMR (376.46 MHz, $CDCl_3$) δ (ppm): 62.48 (s); HRESIMS (m/z): $[M+H]^+$ Calcd for $C_{25}H_{28}F_3N_2O_3$, 461.20465; found, 461.20395.

4.1.6.12. 4-(2-((6,7-Dimethoxy-2-(4-(trifluoromethyl)phenyl)quinolin-4-yl)oxy)ethyl)morpholine (**14l**). White solid, Yield 63%, m.p. 133–135 °C; IR (KBr, ν cm^{-1}): 3096, 3021 (CH aromatic), 2959, 2920, 2882 (CH aliphatic), 1591, 1566, 1510 (C=C aromatic); 1H NMR (400 MHz, $CDCl_3$) δ (ppm): 2.67 (t, 4H, morpholinyl CH_2-N , $J = 4.6$ Hz), 3 (t, 2H, CH_2-N , $J = 5.8$ Hz), 3.74 (t, 4H, morpholinyl $2CH_2-O$, $J = 4.6$ Hz), 4.02 (s, 3H, OCH_3), 4.04 (s, 3H, OCH_3), 4.42 (t, 2H, CH_2-O , $J = 5.8$ Hz), 7.09 (s, 1H, vinyl CH), 7.39 (s, 1H, phenyl CH), 7.44 (s, 1H, phenyl CH), 7.73 (d, 2H, CF_3 -phenyl $2CH$, $J = 8.2$ Hz), 8.16 (d, 2H, CF_3 -phenyl $2CH$, $J = 8.2$ Hz); ^{13}C NMR (100 MHz, $CDCl_3$) δ (ppm): 54.21, 56.00, 56.13, 57.32, 66.65, 66.99, 97.69, 99.67, 108.32, 115.14, 124.25 (CF_3 , q, $J = 271.4$ Hz), 125.61 ($CH-C-CF_3$, q, $J = 3.7$ Hz),

127.53, 130.66 (CH-C-F₃, q, J = 32.3 Hz), 143.81, 146.30, 149.42, 152.94, 155.18, 160.91; ¹⁹F NMR (376.46 MHz, CDCl₃) δ (ppm): 62.49 (s); HRESIMS (m/z): [M+H]⁺ Calcd for C₂₄H₂₆F₃N₂O₄, 463.18392; found, 463.18341.

4.1.6.13. 6,7-Dimethoxy-4-(3-(pyrrolidin-1-yl)propoxy)-2-(4-(trifluoromethyl)phenyl)quinoline (**14m**). White solid, Yield 88%, m.p. 126–128 °C; IR (KBr, ν cm⁻¹): 3084, 3067 (CH aromatic), 2994, 2967, 2944, 2874 (CH aliphatic), 1593, 1561, 1508 (C=C aromatic); ¹H NMR (400 MHz, CDCl₃) δ (ppm): 1.81 (p, 4H, pyrrolidinyl 2CH₂, J = 3.3 Hz), 0.2.20 (p, 2H, CH₂, J = 6.9 Hz), 2.56 (p, 4H, pyrrolidinyl 2CH₂-N, J = 3.3 Hz), 2.72 (t, 2H, CH₂-N, J = 7.3 Hz), 4.02 (s, 3H, OCH₃), 4.03 (s, 3H, OCH₃), 4.35 (t, 2H, CH₂-O, J = 6.4 Hz), 7.11 (s, 1H, vinyl CH), 7.41 (s, 1H, phenyl CH), 7.43 (s, 1H, phenyl CH), 7.73 (d, 2H, CF₃-phenyl 2CH, J = 8.1 Hz), 8.16 (d, 2H, CF₃-phenyl 2CH, J = 8.1 Hz); ¹³C NMR (100 MHz, CDCl₃) δ (ppm): 23.48, 28.68, 53.08, 54.32, 56.07, 56.11, 66.90, 97.74, 99.74, 108.29, 115.22, 124.26 (CF₃, q, J = 272.1 Hz), 125.56 (CH-C-F₃, q, J = 3.5 Hz), 127.56, 130.58 (CH-C-F₃, q, J = 32.4 Hz), 143.93, 146.24, 149.31, 152.84, 155.23, 161.24; ¹⁹F NMR (376.46 MHz, CDCl₃) δ (ppm): 62.47 (s); HRESIMS (m/z): [M+H]⁺ Calcd for C₂₅H₂₈F₃N₂O₃, 461.20465; found, 461.20425.

4.1.6.14. 1-(3-((6,7-Dimethoxy-2-(4-(trifluoromethyl)phenyl)quinolin-4-yl)oxy)propyl)piperidin-4-ol (**14n**). White solid, Yield 88%, m.p. 173–175 °C; IR (KBr, ν cm⁻¹): 3392 (OH), 3000 (CH aromatic), 2935 (CH aliphatic), 1590, 1560, 1508 (C=C aromatic); ¹H NMR (400 MHz, CDCl₃) δ (ppm): 1.56–1.64 (m, 2H, piperidinyl 2CHH'), 1.74 (br s, 1H, OH), 1.88–1.92 (m, 2H, piperidinyl 2CHH'), 2.13–2.22 (m, 4H, piperidinyl 2CHH'-N and CH₂), 2.61 (t, 2H, CH₂-N, J = 7.3 Hz), 2.82 (t, 2H, piperidinyl 2CHH'-N, J = 5.8 Hz), 3.69–3.75 (m, 1H, piperidinyl CH-OH), 4.03 (s, 3H, OCH₃), 4.04 (s, 3H, OCH₃), 4.33 (t, 2H, CH₂-O, J = 6.4 Hz), 7.09 (s, 1H, vinyl CH), 7.40 (s, 1H, phenyl CH), 7.44 (s, 1H, phenyl CH), 7.73 (d, 2H, CF₃-phenyl 2CH, J = 8.2 Hz), 8.16 (d, 2H, CF₃-phenyl 2CH, J = 8.2 Hz); ¹³C NMR (100 MHz, CDCl₃) δ (ppm): 26.90, 34.47, 51.20, 54.99, 56.08, 56.12, 66.81, 67.85, 97.72, 99.69, 108.30, 115.20, 124.27 (CF₃, q, J = 272.7 Hz), 125.59 (CH-C-F₃, q, J = 3.8 Hz), 127.59, 130.62 (CH-C-F₃, q, J = 32.7 Hz), 143.93, 146.26, 149.34, 152.87, 155.28, 161.20; ¹⁹F NMR (376.46 MHz, CDCl₃) δ (ppm): 62.48 (s); HRESIMS (m/z): [M+H]⁺ Calcd for C₂₆H₃₀F₃N₂O₄, 491.21522; found, 491.21472.

4.1.6.15. 6,7-Dimethoxy-4-(3-(piperidin-1-yl)propoxy)-2-(4-(trifluoromethyl)phenyl)quinoline (**14o**). White solid, Yield 83%, m.p. 109–111 °C; IR (KBr, ν cm⁻¹): 3094, 3006 (CH aromatic), 2939, 2857 (CH aliphatic), 1590, 1561, 1509 (C=C aromatic); ¹H NMR (400 MHz, CDCl₃) δ (ppm): 1.46 (t, 2H, piperidinyl CH₂, J = 5.6 Hz), 1.60 (p, 4H, piperidinyl 2CH₂, J = 5.6 Hz), 2.16 (p, 2H, CH₂, J = 6.9 Hz), 2.43 (br s, 4H, piperidinyl 2CH₂-N), 2.57 (t, 2H, CH₂-N, J = 7.4 Hz), 4.02 (s, 3H, OCH₃), 4.03 (s, 3H, OCH₃), 4.31 (t, 2H, CH₂-O, J = 6.4 Hz), 7.08 (s, 1H, vinyl CH), 7.40 (s, 1H, phenyl CH), 7.43 (s, 1H, phenyl CH), 7.72 (d, 2H, CF₃-phenyl 2CH, J = 8.2 Hz), 8.16 (d, 2H, CF₃-phenyl 2CH, J = 8.2 Hz); ¹³C NMR (100 MHz, CDCl₃) δ (ppm): 24.40, 25.99, 26.67, 54.76, 55.92, 56.06, 56.10, 66.99, 97.70, 99.72, 108.28, 115.23, 124.26 (CF₃, q, J = 272.1 Hz), 125.56 (CH-C-F₃, q, J = 3.8 Hz), 127.57, 130.58 (CH-C-F₃, q, J = 32.4 Hz), 143.95, 146.24, 149.31, 152.84, 155.23, 161.23; ¹⁹F NMR (376.46 MHz, CDCl₃) δ (ppm): 62.47 (s); HRESIMS (m/z): [M+H]⁺ Calcd for C₂₆H₃₀F₃N₂O₃, 475.22030; found, 475.22006.

4.1.6.16. 4-(3-((6,7-Dimethoxy-2-(4-(trifluoromethyl)phenyl)quinolin-4-yl)oxy)propyl)morpholine (**14p**). White solid, Yield 79%, m.p. 105–107 °C; IR (KBr, ν cm⁻¹): 3096, 3000 (CH aromatic), 2958, 2939, 2868, 2853 (CH aliphatic), 1591, 1565, 1508 (C=C aromatic); ¹H NMR (400 MHz, CDCl₃) δ (ppm): 2.17 (p, 2H, CH₂, J = 6.8 Hz), 2.50 (t, 4H, morpholinyl CH₂-N, J = 4.4 Hz), 2.62 (t, 2H, CH₂-N,

J = 7.2 Hz), 3.73 (t, 4H, morpholinyl 2CH₂-O, J = 4.4 Hz), 4.03 (s, 3H, OCH₃), 4.04 (s, 3H, OCH₃), 4.35 (t, 2H, CH₂-O, J = 6.4 Hz), 7.10 (s, 1H, vinyl CH), 7.40 (s, 1H, phenyl CH), 7.44 (s, 1H, phenyl CH), 7.74 (d, 2H, CF₃-phenyl 2CH, J = 8.2 Hz), 8.16 (d, 2H, CF₃-phenyl 2CH, J = 8.2 Hz); ¹³C NMR (100 MHz, CDCl₃) δ (ppm): 26.25, 53.84, 55.49, 56.07, 56.13, 66.59, 66.96, 97.69, 99.65, 108.33, 115.17, 124.25 (CF₃, q, J = 272 Hz), 125.59 (CH-C-F₃, q, J = 3.7 Hz), 127.57, 130.64 (CH-C-F₃, q, J = 32.4 Hz), 143.92, 146.28, 149.36, 152.89, 155.25, 161.16; ¹⁹F NMR (376.46 MHz, CDCl₃) δ (ppm): 62.48 (s); HRESIMS (m/z): [M+H]⁺ Calcd for C₂₅H₂₈F₃N₂O₄, 477.19957; found, 477.19943.

4.1.7. General procedure for synthesis of the aroyl derivatives (16a-c)

The aroyl derivatives **16a-c** were synthesized by reaction of the 2-aminoacetophenone derivative **9** with the appropriate aroyl chloride **15a-c** using the same procedure as **11a, b**.

4.1.7.1. N-(2-Acetyl-4,5-dimethoxyphenyl)furan-2-carboxamide (**16a**). Yellow solid, yield 72%, m.p. 162–164 °C; IR (KBr, ν cm⁻¹): 3138 (NH-C=O), 3009, 3001 (CH aromatic), 2968, 2939, 2856 (CH aliphatic), 1670 (CH₃C=O), 1635 (NH-C=O), 1562, 1521 (C=C aromatic); ¹H NMR (400 MHz, CDCl₃) δ (ppm): 2.64 (s, 3H, CH₃), 3.90 (s, 3H, OCH₃), 3.99 (s, 3H, OCH₃), 6.54 (dd, 1H, furyl CH, J = 3.5, 1.7 Hz), 7.21 (dd, 1H, furyl CH, J = 3.5, 0.8 Hz), 7.29 (s, 1H, phenyl CH), 7.60 (dd, 1H, furyl CH, J = 1.7, 0.8 Hz), 8.65 (s, 1H, phenyl CH), 12.92 (s, 1H, NH); ¹³C NMR (100 MHz, CDCl₃) δ (ppm): 28.31, 56.20, 56.38, 103.59, 112.29, 113.74, 114.63, 115.21, 137.52, 143.74, 145.01, 148.28, 154.64, 157.19 (C=O), 200.81 (C=O); HRESIMS (m/z): [M+Na]⁺ Calcd for C₁₅H₁₅NO₅Na, 312.08424; found, 312.08429.

4.1.7.2. N-(2-Acetyl-4,5-dimethoxyphenyl)thiophene-2-carboxamide (**16b**). Yellow solid, yield 72%, m.p. 163–165 °C; IR (KBr, ν cm⁻¹): 3115 (NH-C=O), 3082, 3003, 3000 (CH aromatic), 2938, 2916, 2852 (CH aliphatic), 1654 (CH₃C=O), 1635 (NH-C=O), 1596, 1522 (C=C aromatic); ¹H NMR (400 MHz, CDCl₃) δ (ppm): 2.64 (s, 3H, CH₃), 3.90 (s, 3H, OCH₃), 3.99 (s, 3H, OCH₃), 7.14 (dd, 1H, thiophene CH, J = 5, 3.8 Hz), 7.29 (s, 1H, phenyl CH), 7.56 (dd, 1H, thiophene CH, J = 5, 1.1 Hz), 7.81 (dd, 1H, thiophene CH, J = 3.8, 1.1 Hz), 8.63 (s, 1H, phenyl CH), 12.98 (s, 1H, NH); ¹³C NMR (100 MHz, CDCl₃) δ (ppm): 28.37, 56.24, 56.40, 103.33, 113.77, 114.22, 128.01, 128.65, 131.27, 138.10, 140.45, 143.67, 154.89, 160.90 (C=O), 201.13 (C=O); HRESIMS (m/z): [M+Na]⁺ Calcd for C₁₅H₁₅NO₄Na, 328.06140; found, 328.06149.

4.1.7.3. N-(2-Acetyl-4,5-dimethoxyphenyl)thiophene-3-carboxamide (**16c**). Yellow solid, yield 65%, m.p. 178–180 °C; IR (KBr, ν cm⁻¹): 3198 (NH-C=O), 3099, 3089, 3033, 3006 (CH aromatic), 2953, 2932, 2910, 2850 (CH aliphatic), 1655 (CH₃C=O), 1633 (NH-C=O), 1594, 1519 (C=C aromatic); ¹H NMR (400 MHz, CDCl₃) δ (ppm): 2.65 (s, 3H, CH₃), 3.91 (s, 3H, OCH₃), 4.01 (s, 3H, OCH₃), 7.30 (s, 1H, phenyl CH), 7.39 (dd, 1H, thiophene CH, J = 5.1, 3 Hz), 7.67 (dd, 1H, thiophene CH, J = 5.1, 1.3 Hz), 8.13 (dd, 1H, thiophene CH, J = 3, 1.3 Hz), 8.69 (s, 1H, phenyl CH), 12.87 (s, 1H, NH); ¹³C NMR (100 MHz, CDCl₃) δ (ppm): 28.41, 56.24, 56.42, 103.35, 113.83, 114.29, 126.38, 126.68, 129.44, 138.33, 138.36, 143.62, 154.91, 161.72 (C=O), 201.10 (C=O); HRESIMS (m/z): [M+Na]⁺ Calcd for C₁₅H₁₅NO₄Na, 328.06140; found, 328.06122.

4.1.8. General procedure for synthesis of the quinolones (17a-c)

The quinolones **17a-c** were prepared using the same procedures as **12a, b**.

4.1.8.1. 2-(Furan-2-yl)-6,7-dimethoxyquinolin-4(1H)-one (**17a**). Yellow solid, yield 61%, m.p. > 250 °C; IR (KBr, ν cm⁻¹): 3403 (NH), 3099, 3077, 3039, 3000 (CH aromatic), 2946, 2913 (CH aliphatic),

1640 (C=O), 1581, 1541, 1507 (C=C aromatic); ^1H NMR (400 MHz, MeOH-*d*4) δ (ppm): 4.06 (s, 3H, OCH₃), 4.10 (s, 3H, OCH₃), 6.84 (dd, 1H, furyl CH, *J* = 3.6, 1.7 Hz), 7.20 (s, 1H, vinyl CH), 7.49 (s, 1H, phenyl CH), 7.57 (dd, 1H, furyl CH, *J* = 3.6, 0.6 Hz), 7.64 (s, 1H, phenyl CH), 7.84 (s, 1H, NH), 7.97 (dd, 1H, furyl CH, *J* = 1.7, 0.6 Hz); ^{13}C NMR (100 MHz, MeOH-*d*4) δ (ppm): 55.61, 55.88, 98.89, 99.60, 101.76, 113.21, 114.43, 115.27, 136.89, 141.15, 145.41, 147.10, 150.14, 156.51, 169.23 (C=O); HRESIMS (*m/z*): [M+H]⁺ Calcd for C₁₅H₁₄NO₄, 272.09173; found, 272.09195.

4.1.8.2. 6,7-Dimethoxy-2-(thiophen-2-yl)quinolin-4(1H)-one (**17b**). Yellow solid, yield 91%, m.p. > 250 °C; IR (KBr, ν cm⁻¹): 3401 (NH), 3076, 3003 (CH aromatic), 2938, 2902, 2866 (CH aliphatic), 1634 (C=O), 1595, 1519, 1502 (C=C aromatic); ^1H NMR (400 MHz, MeOH-*d*4) δ (ppm): 4.05 (s, 3H, OCH₃), 4.10 (s, 3H, OCH₃), 7.17 (s, 1H, vinyl CH), 7.37 (dd, 1H, thiophene CH, *J* = 5, 3.8 Hz), 7.51 (s, 1H, phenyl CH), 7.61 (s, 1H, phenyl CH), 7.76 (s, 1H, NH), 7.90 (dd, 1H, thiophene CH, *J* = 5, 1.1 Hz), 8.04 (dd, 1H, thiophene CH, *J* = 3.8, 1.1 Hz); ^{13}C NMR (100 MHz, MeOH-*d*4) δ (ppm): 55.78, 56.06, 98.90, 101.46, 101.86, 114.68, 129.22, 130.06, 131.94, 133.71, 137.34, 146.02, 150.50, 156.91, 168.12 (C=O); HRESIMS (*m/z*): [M+H]⁺ Calcd for C₁₅H₁₄NO₃S, 288.06889; found, 288.06918.

4.1.8.3. 6,7-Dimethoxy-2-(thiophen-3-yl)quinolin-4(1H)-one (**17c**). Yellow solid, yield 82%, m.p. > 250 °C; IR (KBr, ν cm⁻¹): 3406 (NH), 3052 (CH aromatic), 2964, 2930 (CH aliphatic), 1635 (C=O), 1507 (C=C aromatic); ^1H NMR (400 MHz, MeOH-*d*4) δ (ppm): 4.01 (s, 3H, OCH₃), 4.05 (s, 3H, OCH₃), 6.89 (s, 1H, vinyl CH), 7.34 (s, 1H, phenyl CH), 7.63 (s, 1H, phenyl CH), 7.76 (dd, 1H, thiophene CH, *J* = 5.1, 1.5 Hz), 7.70 (dd, 1H, thiophene CH, *J* = 5.1, 2.8 Hz), 7.82 (s, 1H, NH), 8.21 (dd, 1H, thiophene CH, *J* = 2.8, 1.5 Hz); ^{13}C NMR (100 MHz, MeOH-*d*4) δ (ppm): 55.44, 55.64, 98.86, 102.61, 103.98, 116.82, 125.57, 126.72, 127.89, 134.26, 136.85, 146.05, 149.07, 155.47, 173.60; HRESIMS (*m/z*): [M+H]⁺ Calcd for C₁₅H₁₄NO₃S, 288.06889; found, 288.06915.

4.1.9. General procedure for synthesis of the key intermediates (18a-c)

The key intermediates **18a-c** were synthesized using the same procedures as **13a-d**.

4.1.9.1. 4-(3-Chloropropoxy)-2-(furan-2-yl)-6,7-dimethoxyquinoline (**18a**). Yellow solid, yield 81%, m.p. 139–141 °C; IR (KBr, ν cm⁻¹): 3092, 3011 (CH aromatic), 2952, 2940, 2879 (CH aliphatic), 1594, 1565, 1510 (C=C aromatic); ^1H NMR (400 MHz, CDCl₃) δ (ppm): 2.43 (p, 2H, CH₂, *J* = 6.1 Hz), 3.82 (t, 2H, CH₂Cl, *J* = 6.3 Hz), 4 (s, 3H, OCH₃), 4.02 (s, 3H, OCH₃), 4.42 (t, 2H, CH₂O, *J* = 5.9 Hz), 6.56 (dd, 1H, furyl CH, *J* = 3.4, 1.7 Hz), 7.11 (s, 1H, furyl CH), 7.12 (s, 1H, vinyl CH), 7.33 (s, 1H, phenyl CH), 7.41 (s, 1H, phenyl CH), 7.57 (dd, 1H, furyl CH, *J* = 1.7, 0.7 Hz); ^{13}C NMR (100 MHz, CDCl₃) δ (ppm): 31.97, 41.34, 56.04, 56.12, 64.98, 95.96, 99.72, 108.13, 108.77, 112.08, 114.86, 143.31, 146.16, 148.44, 148.98, 152.76, 154.09, 160.44; HRESIMS (*m/z*): [M+H]⁺ Calcd for C₁₈H₁₉ClNO₄, 348.09971; found, 348.09988.

4.1.9.2. 4-(3-Chloropropoxy)-6,7-dimethoxy-2-(thiophen-2-yl)quinoline (**18b**). Yellow solid, yield 76%, m.p. 168–170 °C; IR (KBr, ν cm⁻¹): 3071, 3005 (CH aromatic), 2934, 2880 (CH aliphatic), 1591, 1511 (C=C aromatic); ^1H NMR (400 MHz, CDCl₃) δ (ppm): 2.42 (p, 2H, CH₂, *J* = 6.1 Hz), 3.83 (t, 2H, CH₂Cl, *J* = 6.2 Hz), 4 (s, 3H, OCH₃), 4.03 (s, 3H, OCH₃), 4.40 (t, 2H, CH₂O, *J* = 6 Hz), 7.05 (s, 1H, vinyl CH), 7.12 (dd, 1H, thiophene CH, *J* = 5, 3.7 Hz), 7.31 (s, 1H, phenyl CH), 7.37 (s, 1H, phenyl CH), 7.41 (dd, 1H, thiophene CH, *J* = 5, 1.1 Hz), 7.63 (dd, 1H, thiophene CH, *J* = 3.7, 1.1 Hz); ^{13}C NMR (100 MHz, CDCl₃) δ (ppm): 31.97, 41.36, 56.03, 56.12, 64.91, 96.21, 99.76, 108.10, 114.89, 124.68, 127.57, 127.84, 145.94, 146.06, 148.91, 151.61, 152.71,

160.42; HRESIMS (*m/z*): [M+H]⁺ Calcd for C₁₈H₁₉ClNO₃S, 364.07687; found, 364.07706.

4.1.9.3. 4-(3-Chloropropoxy)-6,7-dimethoxy-2-(thiophen-3-yl)quinoline (**18c**). Yellow solid, yield 73%, m.p. 133–135 °C; IR (KBr, ν cm⁻¹): 3089, 3000 (CH aromatic), 2965, 2940, 2914 (CH aliphatic), 1590, 1508 (C=C aromatic); ^1H NMR (400 MHz, CDCl₃) δ (ppm): 2.43 (p, 2H, CH₂, *J* = 6.1 Hz), 3.83 (t, 2H, CH₂Cl, *J* = 6.2 Hz), 4.01 (s, 3H, OCH₃), 4.03 (s, 3H, OCH₃), 4.41 (t, 2H, CH₂O, *J* = 6 Hz), 7.02 (s, 1H, vinyl CH), 7.34 (s, 1H, phenyl CH), 7.40 (s, 1H, phenyl CH), 7.41 (dd, 1H, thiophene CH, *J* = 5, 3 Hz), 7.77 (dd, 1H, thiophene CH, *J* = 5, 1.2 Hz), 7.93 (dd, 1H, thiophene CH, *J* = 3, 1.2 Hz); ^{13}C NMR (100 MHz, CDCl₃) δ (ppm): 31.99, 41.37, 56.04, 56.09, 64.85, 97.67, 99.67, 108.18, 114.72, 123.57, 126.14, 126.72, 143.23, 146.21, 148.90, 152.68, 152.81, 160.53; HRESIMS (*m/z*): [M+H]⁺ Calcd for C₁₈H₁₉ClNO₃S, 364.07687; found, 364.07751.

4.1.10. General procedures for synthesis of the target 4-alkoxy-2-arylquinolines (19a-c)

A mixture of **18a-c** (1 mmol), KI (0.83 g, 5 mmol) and anhydrous K₂CO₃ (1.38 g, 10 mmol) was stirred in dry DMF (20 mL) for 30 min. Then, 4-hydroxymorpholine (1.01 g, 10 mmol) was added to the mixture. The reaction mixture was refluxed at 90 °C for 12 h, then poured into ice water (50 mL). The precipitated solid (**19b, c**) was filtered off, washed with water then hexane. For **19a**, the aqueous layer was extracted with Ethyl acetate (50 mL × 3), then the organic layers were collected and washed with water and brine. The organic layer was dried over anhydrous Na₂SO₄, then evaporated under vacuum. The products **19a-c** were purified by silica gel column chromatography using DCM/MeOH.

4.1.10.1. 1-(3-((2-(Furan-2-yl)-6,7-dimethoxyquinolin-4-yl)oxy)propyl)piperidin-4-ol (**19a**). Yellow solid, yield 75%, m.p. 165–167 °C; IR (KBr, ν cm⁻¹): 3416 (OH), 3007 (CH aromatic), 2929 (CH aliphatic), 1589, 1560, 1509 (C=C aromatic); ^1H NMR (400 MHz, CDCl₃) δ (ppm): 1.57–1.66 (m, 2H, piperidiny 2CHH'), 1.76 (br s, 1H, OH), 1.89–1.94 (m, 2H, piperidiny 2CHH'), 2.12–2.22 (m, 4H, piperidiny 2CHH'-N and CH₂), 2.60 (t, 2H, CH₂-N, *J* = 7.3 Hz), 2.82 (t, 2H, piperidiny 2CHH'-N, *J* = 5.8 Hz), 3.69–3.75 (m, 1H, piperidiny CH-OH), 4 (s, 3H, OCH₃), 4.01 (s, 3H, OCH₃), 4.31 (t, 2H, CH₂-O, *J* = 6.4 Hz), 6.55 (dd, 1H, furyl CH, *J* = 3.5, 1.7 Hz), 7.10 (s, 1H, vinyl CH), 7.12 (dd, 1H, furyl CH, *J* = 3.5, 0.5 Hz), 7.36 (s, 1H, phenyl CH), 7.40 (s, 1H, phenyl CH), 7.56 (dd, 1H, furyl CH, *J* = 1.7, 0.5 Hz); ^{13}C NMR (100 MHz, CDCl₃) δ (ppm): 26.88, 34.48, 51.20, 55.03, 56.03, 56.10, 66.78, 67.93, 95.96, 99.88, 108.09, 108.67, 112.06, 115.02, 143.24, 146.12, 148.49, 148.88, 152.68, 154.21, 160.81; HRESIMS (*m/z*): [M+H]⁺ Calcd for C₂₃H₂₉N₂O₅, 413.20710; found, 413.20676.

4.1.10.2. 1-(3-((6,7-Dimethoxy-2-(thiophen-2-yl)quinolin-4-yl)oxy)propyl)piperidin-4-ol (**19b**). Yellow solid, yield 86%, m.p. 88–90 °C; IR (KBr, ν cm⁻¹): 3400 (OH), 3091, 3000 (CH aromatic), 2935 (CH aliphatic), 1589, 1507 (C=C aromatic); ^1H NMR (400 MHz, CDCl₃) δ (ppm): 1.56–1.65 (m, 2H, piperidiny 2CHH'), 1.73 (br s, 1H, OH), 1.88–1.94 (m, 2H, piperidiny 2CHH'), 2.12–2.22 (m, 4H, piperidiny 2CHH'-N and CH₂), 2.60 (t, 2H, CH₂-N, *J* = 7.3 Hz), 2.82 (t, 2H, piperidiny 2CHH'-N, *J* = 5.8 Hz), 3.69–3.75 (m, 1H, piperidiny CH-OH), 4 (s, 3H, OCH₃), 4.02 (s, 3H, OCH₃), 4.30 (t, 2H, CH₂-O, *J* = 6.4 Hz), 7.04 (s, 1H, vinyl CH), 7.12 (dd, 1H, thiophene CH, *J* = 5, 3.7 Hz), 7.35 (s, 1H, phenyl CH), 7.36 (s, 1H, phenyl CH), 7.40 (dd, 1H, thiophene CH, *J* = 5, 1.1 Hz), 7.63 (dd, 1H, thiophene CH, *J* = 3.7, 1.1 Hz); ^{13}C NMR (100 MHz, CDCl₃) δ (ppm): 26.89, 34.48, 51.21, 55.03, 56.02, 56.11, 66.72, 67.89, 96.23, 99.91, 108.06, 115.04, 124.62, 127.48, 127.80, 146.01, 146.05, 148.81, 151.65, 152.64, 160.79; HRESIMS (*m/z*): [M+H]⁺ Calcd for C₂₃H₂₉N₂O₄S, 429.18425; found,

429.18414.

4.1.10.3. 1-(3-((6,7-Dimethoxy-2-(thiophen-3-yl)quinolin-4-yl)oxy)propyl)piperidin-4-ol (**19c**). Yellow solid, yield 65%, m.p. 158–160 °C; IR (KBr, ν cm^{-1}): 3401 (OH), 3100, 3000 (CH aromatic), 2931 (CH aliphatic), 1591, 1509 (C=C aromatic); ^1H NMR (400 MHz, CDCl_3) δ (ppm): 1.56–1.65 (m, 2H, piperidinyl 2CHH'), 1.72 (br s, 1H, OH), 1.89–1.93 (m, 2H, piperidinyl 2CHH'), 2.12–2.22 (m, 4H, piperidinyl 2CHH'-N and CH_2), 2.60 (t, 2H, $\text{CH}_2\text{-N}$, $J = 7.3$ Hz), 2.82 (t, 2H, piperidinyl 2CHH'-N, $J = 5.8$ Hz), 3.69–3.75 (m, 1H, piperidinyl CH-OH), 4.01 (s, 3H, OCH_3), 4.03 (s, 3H, OCH_3), 4.30 (t, 2H, $\text{CH}_2\text{-O}$, $J = 6.4$ Hz), 7 (s, 1H, vinyl CH), 7.37 (s, 1H, phenyl CH), 7.39 (s, 1H, phenyl CH), 7.41 (dd, 1H, thiophene CH, $J = 5, 3$ Hz), 7.76 (dd, 1H, thiophene CH, $J = 5, 1.2$ Hz), 7.92 (dd, 1H, thiophene CH, $J = 3, 1.2$ Hz); ^{13}C NMR (100 MHz, CDCl_3) δ (ppm): 26.91, 34.48, 51.21, 55.04, 56.03, 56.07, 66.67, 67.88, 97.69, 99.83, 108.13, 114.86, 123.50, 126.08, 126.76, 143.35, 146.15, 148.80, 152.60, 152.87, 160.89; HRE-SIMS (m/z): $[\text{M}+\text{H}]^+$ Calcd for $\text{C}_{23}\text{H}_{29}\text{N}_2\text{O}_4\text{S}$, 429.18425; found, 429.18414.

4.2. *In vitro* anticancer activity

The cytotoxicity *in vitro* assay was conducted at National Cancer Institute (NCI), Bethesda, USA against 59 cancer cell lines, as reported earlier [64,65]. The one-dose data were reported as a mean graph of the percent growth of treated cells. The number reported for the one-dose assay was growth relative to the no-drug control and relative to the time zero number of cells. This allowed detection of both growth inhibition (values between 0 and 100) and lethality (values less than 0). For example, a value of 100 means no growth inhibition. A value of 40 would mean 60% growth inhibition. A value of 0 means no net growth over the course of the experiment. A value of -40 would mean 40% lethality. A value of -100 means all cells were dead.

The human tumor cell lines of the cancer screening panel were grown in RPMI 1640 medium containing 5% fetal bovine serum and 2 mM L-glutamine. For a typical screening experiment, cells were inoculated into 96 well microtiter plates in 100 μL at plating densities ranging from 5000 to 40,000 cells/well depending on the doubling time of individual cell lines. After cell inoculation, the microtiter plates were incubated at 37 °C, 5% CO_2 , 95% air and 100% relative humidity for 24 h prior to addition of experimental drugs. After 24 h, two plates of each cell line were fixed *in situ* with TCA, to represent a measurement of the cell population for each cell line at the time of drug addition (Tz). Experimental drugs were solubilized in dimethyl sulfoxide at 400-fold the desired final maximum test concentration and stored frozen prior to use. At the time of drug addition, an aliquot of frozen concentrate was thawed and diluted to twice the desired final maximum test concentration with complete medium containing 50 $\mu\text{g}/\text{mL}$ gentamicin. Additional four, 10-fold or $\frac{1}{2}$ log serial dilutions were made to provide a total of five drug concentrations plus control. Aliquots of 100 μL of these different drug dilutions were added to the appropriate microtiter wells already containing 100 μL of medium, resulting in the required final drug concentrations. Following drug addition, the plates were incubated for an additional 48 h at 37 °C, 5% CO_2 , 95% air, and 100% relative humidity. For adherent cells, the assay was terminated by the addition of cold TCA. Cells were fixed *in situ* by the gentle addition of 50 μL of cold 50% (w/v) TCA (final concentration, 10% TCA) and incubated for 60 min at 4 °C. The supernatant was discarded, and the plates were washed five times with tap water and air dried. Sulforhodamine B (SRB) solution (100 μL) at 0.4% (w/v) in 1% acetic acid was added to each well, and plates were incubated for 10 min at room temperature. After staining, unbound dye was removed by washing five times with 1% acetic acid and the

plates were air dried. Bound stain was subsequently solubilized with 10 mM trizma base, and the absorbance was read on an automated plate reader at a wavelength of 515 nm. For suspension cells, the methodology was the same except that the assay was terminated by fixing settled cells at the bottom of the wells by gently adding 50 μL of 80% TCA (final concentration, 16% TCA). Using the seven absorbance measurements [time zero, (Tz), control growth, (C), and test growth in the presence of drug at the five concentration levels (Ti)], the percentage growth was calculated at each of the drug concentrations levels. Percentage growth inhibition was calculated as:

$$[(\text{Ti}-\text{Tz})/(\text{C}-\text{Tz})] \times 100 \text{ for concentrations for which } \text{Ti} > \text{Tz}$$

$$[(\text{Ti}-\text{Tz})/\text{Tz}] \times 100 \text{ for concentrations for which } \text{Ti} < \text{Tz}$$

Three dose response parameters were calculated for each experimental agent. Growth inhibition of 50% (GI_{50}) was calculated from $[(\text{Ti}-\text{Tz})/(\text{C}-\text{Tz})] \times 100 = 50$, which is the drug concentration resulting in a 50% reduction in the net protein increase (as measured by SRB staining) in control cells during the drug incubation. The drug concentration resulting in total growth inhibition (TGI) was calculated from $\text{Ti} = \text{Tz}$. The LC_{50} (concentration of drug resulting in a 50% reduction in the measured protein at the end of the drug treatment as compared to that at the beginning) indicating a net loss of cells following treatment was calculated from $[(\text{Ti}-\text{Tz})/\text{Tz}] \times 100 = -50$.

4.3. Topoisomerase I-mediated DNA cleavage assay

A 3'-[^{32}P]-labeled 117-bp DNA substrate oligonucleotide was prepared as described previously [55]. Radiolabeled DNA was incubated with recombinant human TOP1 in 20 μL reaction buffer (10 mmol/L Tris-HCl, pH 7.5, 50 mmol/L KCl, 5 mmol/L MgCl_2 , 0.1 mmol/L EDTA, and 15 $\mu\text{g}/\text{mL}$ BSA) at 30 °C for 20 min in the presence of the indicated drug concentrations. Reactions were terminated by adding SDS (0.5% final concentration) followed by the addition of two volumes of loading dye (80% formamide, 10 mmol/L sodium hydroxide, 1 mmol/L sodium EDTA, 0.1% xylene cyanol, and 0.1% bromophenol blue). Aliquots of reaction mixtures were subjected to 16% denaturing PAGE. Gels were dried and visualized by using PhosphorImager and Image Quant software (Molecular Dynamics).

Declaration of competing interest

The authors have declared no conflict of interest.

Acknowledgement

Mostafa M. Elbadawi was supported by MEXT scholarship provided by the Ministry of Education, Culture, Sports, Science and Technology of Japan (scholarship no. 182582). Yves Pommier and Keli K. Agama are supported by the Center for Cancer Research, the Intramural Program of the National Cancer Institute (Z01-BC-006161). The authors are thankful to Developmental Therapeutics Program (DTP) of the National Cancer Institute (NCI) for *in vitro* anticancer screening of the newly synthesized compounds. Also, the authors are grateful to Dr. Sayaka Hatano for help in X-ray crystallography. Moreover, we would like to thank Professor Norimatsu Morioka and Dr. Yoki Nakamura (Department of Pharmacology, Graduate School of Biomedical and Health Sciences, Hiroshima University, Japan) for their informative discussions.

Appendix A. Supplementary data

Supplementary data to this article can be found online at <https://doi.org/10.1016/j.ejmech.2021.113261>.

References

- [1] C.K. Peng, T. Zeng, X.J. Xu, Y.Q. Chang, W. Hou, K. Lu, H. Lin, P.H. Sun, J. Lin, W.M. Chen, Novel 4-(4-substituted amidobenzyl)furan-2(5H)-one derivatives as topoisomerase I inhibitors, *Eur. J. Med. Chem.* 127 (2017) 187–199, <https://doi.org/10.1016/j.ejmech.2016.12.035>.
- [2] J. Kovvuri, B. Nagaraju, V.L. Nayak, R. Akunuri, M.P.N. Rao, A. Ajitha, N. Nagesh, A. Kamal, Design, synthesis and biological evaluation of new β -carboline-bisindole compounds as DNA binding, photocleavage agents and topoisomerase I inhibitors, *Eur. J. Med. Chem.* 143 (2018) 1563–1577, <https://doi.org/10.1016/j.ejmech.2017.10.054>.
- [3] F. Bray, J. Ferlay, I. Soerjomataram, R.L. Siegel, L.A. Torre, A. Jemal, Global cancer statistics 2018: GLOBOCAN estimates of incidence and mortality worldwide for 36 cancers in 185 countries, *CA, Cancer J. Clin.* 68 (2018) 394–424, <https://doi.org/10.3322/caac.21492>.
- [4] M. Pannala, S. Kher, N. Wilson, J. Gaudette, I. Sircar, S.H. Zhang, A. Bakhirev, G. Yang, P. Yuen, F. Gorcsan, N. Sakurai, M. Barbosa, J.F. Cheng, Synthesis and structure-activity relationship of 4-(2-aryl-cyclopropylamino)-quinoline-3-carbonitriles as EGFR tyrosine kinase inhibitors, *Bioorg. Med. Chem. Lett* 17 (2007) 5978–5982, <https://doi.org/10.1016/j.bmcl.2007.07.071>.
- [5] Q.D. You, Z.Y. Li, C.H. Huang, Q. Yang, X.J. Wang, Q.L. Guo, X.G. Chen, X.G. He, T.K. Li, J.W. Chern, Discovery of a novel series of quinolone and naphthyridine derivatives as potential topoisomerase I inhibitors by scaffold modification, *J. Med. Chem.* 52 (2009) 5649–5661, <https://doi.org/10.1021/jm900469e>.
- [6] V.G. Pawar, M.L. Sos, H.B. Rode, M. Rabiller, S. Heynck, W.A.L. Van Otterlo, R.K. Thomas, D. Rauh, Synthesis and biological evaluation of 4-anilinoquinolines as potent inhibitors of epidermal growth factor receptor, *J. Med. Chem.* 53 (2010) 2892–2901, <https://doi.org/10.1021/jm901877j>.
- [7] A. Weyesa, E. Mulugeta, Recent advances in the synthesis of biologically and pharmaceutically active quinoline and its analogues: a review, *RSC Adv.* 10 (2020) 20784–20793, <https://doi.org/10.1039/d0ra03763j>.
- [8] O. Afzal, S. Kumar, M.R. Haider, M.R. Ali, R. Kumar, M. Jaggi, S. Bawa, A review on anticancer potential of bioactive heterocycle quinoline, *Eur. J. Med. Chem.* 97 (2015) 871–910, <https://doi.org/10.1016/j.ejmech.2014.07.044>.
- [9] T. Felicetti, R. Cannalire, D. Pietrella, G. Latacz, A. Lubelska, G. Manfroni, M.L. Barreca, S. Massari, O. Tabarrini, K. Kieć-Kononowicz, B.D. Schindler, G.W. Kaatz, V. Cecchetti, S. Sabatini, 2-Phenylquinoline S. aureus NorA efflux pump inhibitors: evaluation of the importance of methoxy group introduction, *J. Med. Chem.* 61 (2018) 7827–7848, <https://doi.org/10.1021/acs.jmedchem.8b00791>.
- [10] T. Van de Walle, M. Boone, J. Van Puyvelde, J. Combrinck, P.J. Smith, K. Chibale, S. Mangelinckx, M. D'hooghe, Synthesis and biological evaluation of novel quinoline-piperidine scaffolds as antiparasitoidium agents, *Eur. J. Med. Chem.* 198 (2020), 112330, <https://doi.org/10.1016/j.ejmech.2020.112330>.
- [11] A. Singh, M. Kalamuddin, M. Maqbool, A. Mohammed, P. Malhotra, N. Hoda, Quinoline carboxamide core moiety-based compounds inhibit P. falciparum falcipain-2: design, synthesis and antimalarial efficacy studies, *Bioorg. Chem.* (2020) 104514, <https://doi.org/10.1016/j.bioorg.2020.104514>.
- [12] R.K. Arafa, G.H. Hegazy, G.A. Piazza, A.H. Abadi, Synthesis and in vitro antiproliferative effect of novel quinoline-based potential anticancer agents, *Eur. J. Med. Chem.* 63 (2013) 826–832, <https://doi.org/10.1016/j.ejmech.2013.03.008>.
- [13] Y.L. Chen, C.J. Huang, Z.Y. Huang, C.H. Tseng, F.S. Chang, S.H. Yang, S.R. Lin, C.C. Tzeng, Synthesis and antiproliferative evaluation of certain 4-anilino-8-methoxy-2-phenylquinoline and 4-anilino-8-hydroxy-2-phenylquinoline derivatives, *Bioorg. Med. Chem.* 14 (2006) 3098–3105, <https://doi.org/10.1016/j.bmcl.2005.12.017>.
- [14] X.Y. Jin, H. Chen, D.D. Li, A.L. Li, W.Y. Wang, W. Gu, Design, synthesis, and anticancer evaluation of novel quinoline derivatives of ursolic acid with hydrazide, oxadiazole, and thiadiazole moieties as potent MEK inhibitors, *J. Enzym. Inhib. Med. Chem.* 34 (2019) 955–972, <https://doi.org/10.1080/14756366.2019.1605364>.
- [15] S. Li, C. Guo, X. Sun, Y. Li, H. Zhao, D. Zhan, M. Lan, Y. Tang, Synthesis and biological evaluation of quinazoline and quinoline bearing 2,2,6,6-tetramethylpiperidine-N-oxyl as potential epidermal growth factor receptor (EGFR) tyrosine kinase inhibitors and EPR bio-probe agents, *Eur. J. Med. Chem.* 49 (2012) 271–278, <https://doi.org/10.1016/j.ejmech.2012.01.021>.
- [16] V.R. Solomon, H. Lee, Quinoline as a privileged scaffold in cancer drug discovery, *Curr. Med. Chem.* 18 (10) (2011) 1488–1508, <https://doi.org/10.2174/092986711795328382>.
- [17] E.A. Abdelsalam, W.A. Zaghary, K.M. Amin, N.A. Abou Taleb, A.A.I. Mekawey, W.M. Eldehna, H.A. Abdel-Aziz, S.F. Hammad, Synthesis and in vitro anticancer evaluation of some fused indazoles, quinazolines and quinolines as potential EGFR inhibitors, *Bioorg. Chem.* 89 (2019) 102985, <https://doi.org/10.1016/j.bioorg.2019.102985>.
- [18] M.M. Al-Sanea, A. Elkamhaway, S. Paik, S. Bua, S. Ha Lee, M.A. Abdelgawad, E.J. Roh, W.M. Eldehna, C.T. Supuran, Synthesis and biological evaluation of novel 3-(quinolin-4-ylamino)benzenesulfonamide as carbonic anhydrase isoforms I and II inhibitors, *J. Enzym. Inhib. Med. Chem.* 34 (2019) 1457–1464, <https://doi.org/10.1080/14756366.2019.1652282>.
- [19] K. Li, Y. Li, D. Zhou, Y. Fan, H. Guo, T. Ma, J. Wen, D. Liu, L. Zhao, Synthesis and biological evaluation of quinoline derivatives as potential anti-prostate cancer agents and Pim-1 kinase inhibitors, *Bioorg. Med. Chem.* 24 (2016) 1889–1897, <https://doi.org/10.1016/j.bmc.2016.03.016>.
- [20] S. Li, L. Hu, J. Li, J. Zhu, F. Zeng, Q. Huang, L. Qiu, R. Du, R. Cao, Design, synthesis, structure-activity relationships and mechanism of action of new quinoline derivatives as potential antitumor agents, *Eur. J. Med. Chem.* 162 (2019) 666–678, <https://doi.org/10.1016/j.ejmech.2018.11.048>.
- [21] X. Nan, H.J. Li, S.B. Fang, Q.Y. Li, Y.C. Wu, Structure-based discovery of novel 4-(2-fluorophenoxy)quinoline derivatives as c-Met inhibitors using isocyanide-involved multicomponent reactions, *Eur. J. Med. Chem.* 193 (2020) 112241, <https://doi.org/10.1016/j.ejmech.2020.112241>.
- [22] C. Alonso, M. Fuentes, E. Martín-Encinas, A. Selas, G. Rubiales, C. Tesauro, B.K. Knudssen, F. Palacios, Novel topoisomerase I inhibitors. Syntheses and biological evaluation of phosphorus substituted quinoline derivatives with antiproliferative activity, *Eur. J. Med. Chem.* 149 (2018) 225–237, <https://doi.org/10.1016/j.ejmech.2018.02.058>.
- [23] A. Mazza, E.M. Beccalli, A. Contini, A.N. Garcia-Argaez, L. Dalla Via, M.L. Gelmi, A new scaffold of topoisomerase I inhibitors: design, synthesis and biological evaluation, *Eur. J. Med. Chem.* 124 (2016) 326–339, <https://doi.org/10.1016/j.ejmech.2016.08.045>.
- [24] B. Kundu, S.K. Das, S. Paul Chowdhuri, S. Pal, D. Sarkar, A. Ghosh, A. Mukherjee, D. Bhattacharya, B.B. Das, A. Talukdar, Discovery and mechanistic study of tailor-made quinoline derivatives as topoisomerase 1 poison with potent anticancer activity, *J. Med. Chem.* 62 (2019) 3428–3446, <https://doi.org/10.1021/acs.jmedchem.8b01938>.
- [25] J.C. Wang, Cellular roles of DNA topoisomerases: a molecular perspective, *Nat. Rev. Mol. Cell Biol.* 3 (2002) 430–440, <https://doi.org/10.1038/nrm831>.
- [26] B.L. Staker, M.D. Feese, M. Cushman, Y. Pommier, D. Zembower, L. Stewart, A.B. Burgin, Structures of three classes of anticancer agents bound to the human topoisomerase I-DNA covalent complex, *J. Med. Chem.* 48 (2005) 2336–2345, <https://doi.org/10.1021/jm049146p>.
- [27] Y. Pommier, Topoisomerase I inhibitors: camptothecins and beyond, *Nat. Rev. Canc.* 6 (2006) 789–802, <https://doi.org/10.1038/nrc1977>.
- [28] Y. Pommier, Drugging topoisomerases: lessons and challenges, *ACS Chem. Biol.* 8 (2013) 82–95, <https://doi.org/10.1021/cb300648v>.
- [29] L. Marzi, K. Agama, J. Murai, S. Difilippantonio, A. James, C.J. Peer, W.D. Figg, D. Beck, M.S.A. Elsayed, M. Cushman, Y. Pommier, Novel fluoroindenoisoquinoline non-camptothecin topoisomerase I inhibitors, *Mol. Canc. Therapeut.* 17 (2018) 1694–1704, <https://doi.org/10.1158/1535-7163.MCT-18-0028>.
- [30] W.L. Tang, Y. Zhang, D.X. Hu, H. Yang, Q. Yu, J.W. Chen, K. Agama, Y. Pommier, L.K. An, Synthesis and biological evaluation of 5-aminoethyl benzophenanthridone derivatives as DNA topoisomerase IB inhibitors, *Eur. J. Med. Chem.* 178 (2019) 81–92, <https://doi.org/10.1016/j.ejmech.2019.05.074>.
- [31] P. Majumdar, C. Bathula, S.M. Basu, S.K. Das, R. Agarwal, S. Hati, A. Singh, S. Sen, B.B. Das, Design, synthesis and evaluation of thiohydantoin derivatives as potent topoisomerase I (Top1) inhibitors with anticancer activity, *Eur. J. Med. Chem.* 102 (2015) 540–551, <https://doi.org/10.1016/j.ejmech.2015.08.032>.
- [32] B. Shu, Q. Yu, D. xuan Hu, T. Che, S. shi Zhang, D. Li, Synthesis and biological evaluation of novel indole-pyrazoline hybrid derivatives as potential topoisomerase I inhibitors, *Bioorg. Med. Chem. Lett* 30 (2020), 126925, <https://doi.org/10.1016/j.bmcl.2019.126925>.
- [33] D.E. Beck, W. Lv, M. Abdelmalak, C.B. Plescia, K. Agama, C. Marchand, Y. Pommier, M. Cushman, Synthesis and biological evaluation of new fluorinated and chlorinated indenoisoquinoline topoisomerase I poisons, *Bioorg. Med. Chem.* 24 (2016) 1469–1479, <https://doi.org/10.1016/j.bmc.2016.02.015>.
- [34] A.I. Khodair, M.M. Elbadawi, M.T. Elsaady, K.R.A. Abdellatif, Design, synthesis, molecular docking and cytotoxicity evaluation of some novel 5-arylidene-3-(substituted phenyl)-2-(p-tolylamino)-4-imidazolones, *J. Appl. Pharmaceut. Sci. 7* (2017), <https://doi.org/10.7324/JAPS.2017.70908>, 058–068.
- [35] P.C. Lv, M.S.A. Elsayed, K. Agama, C. Marchand, Y. Pommier, M. Cushman, Design, synthesis, and biological evaluation of potential prodrugs related to the experimental anticancer agent indotecan (LMP400), *J. Med. Chem.* 59 (2016) 4890–4899, <https://doi.org/10.1021/acs.jmedchem.6b00220>.
- [36] A. Thomas, Y. Pommier, Targeting topoisomerase I in the era of precision medicine, *Clin. Canc. Res.* 25 (2019) 6581–6589, <https://doi.org/10.1158/1078-0432.CCR-19-1089>.
- [37] Y. Pommier, E. Leo, H. Zhang, C. Marchand, DNA topoisomerases and their poisoning by anticancer and antibacterial drugs, *Chem. Biol.* 17 (2010) 421–433, <https://doi.org/10.1016/j.chembiol.2010.04.012>.
- [38] J.-M. Yuan, N.-Y. Chen, H.-R. Liao, G.-H. Zhang, X.-J. Li, Z.-Y. Gu, C.-X. Pan, D.-L. Mo, G.-F. Su, 3-(Benzo[d]thiazol-2-yl)-4-aminoquinoline derivatives as novel scaffold topoisomerase I inhibitor via DNA intercalation: design, synthesis, and antitumor activities, *New J. Chem.* (2020) 11203–11214, <https://doi.org/10.1039/c9nj05846j>.
- [39] L.S. Kurtzberg, S. Roth, R. Krumbholz, J. Crawford, C. Bormann, S. Dunham, M. Yao, C. Rouleau, R.G. Bagley, X.J. Yu, F. Wang, S.M. Schmid, E.J. LaVoie, B.A. Teicher, Genz-644282, a novel non-camptothecin topoisomerase I inhibitor for cancer treatment, *Clin. Canc. Res.* 17 (2011) 2777–2787, <https://doi.org/10.1158/1078-0432.CCR-10-0542>.

- [40] F. Coussy, R. El-Botty, S. Château-Joubert, A. Dahmani, E. Montaudon, S. Leboucher, L. Morisset, P. Painsec, L. Sourd, L. Huguët, F. Nemati, J.L. Servely, T. Larcher, S. Vacher, A. Briaux, C. Reyes, P. La Rosa, G. Lucotte, T. Popova, P. Foidart, N.E. Sounni, A. Noel, D. Decaudin, L. Fuhrmann, A. Salomon, F. Reyat, C. Mueller, P. Ter Brugge, J. Jonkers, M.F. Poupon, M.H. Stern, I. Bièche, Y. Pommier, E. Marangoni, BRCAness, SLFN11, and RB1 loss predict response to topoisomerase I inhibitors in triple-negative breast cancers, *Sci. Transl. Med.* 12 (2020) 1–13, <https://doi.org/10.1126/scitranslmed.aax2625>.
- [41] R. Ge, Q. Zhao, Z. Xie, L. Lu, Q. Guo, Z. Li, L. Zhao, Synthesis and biological evaluation of 6-fluoro-3-phenyl-7-piperazinyl quinolone derivatives as potential topoisomerase I inhibitors, *Eur. J. Med. Chem.* 122 (2016) 465–474, <https://doi.org/10.1016/j.ejmech.2016.06.054>.
- [42] K.R.A. Abdellatif, M.M. Elbadawi, M.T. Elsaady, A.A. Abd El-Hafeez, T. Fujimura, S. Kawamoto, A.I. Khodair, Design, synthesis and cytotoxicity evaluation of new 3, 5-disubstituted-2-thioxoimidazolidinones, *Anticancer. Agents Med. Chem.* 18 (2018) 573–582, <https://doi.org/10.2174/1871520618666171129213838>.
- [43] L. Marzi, L. Szabova, M. Gordon, Z.W. Ohler, S.K. Sharan, M.L. Beshiri, M. Etemadi, J. Murai, K. Kelly, Y. Pommier, The indenoisoquinoline TOP1 inhibitors selectively target homologous recombination-deficient and Schlafen 11-positive cancer cells and synergize with olaparib, *Clin. Canc. Res.* 25 (2019) 6206–6216, <https://doi.org/10.1158/1078-0432.CCR-19-0419>.
- [44] G. Zoppioli, M. Regairaz, E. Leo, W.C. Reinhold, S. Varma, A. Ballestrero, J.H. Doroshow, Y. Pommier, Putative DNA/RNA helicase Schlafen-11 (SLFN11) sensitizes cancer cells to DNA-damaging agents, *Proc. Natl. Acad. Sci. U. S. A.* 109 (2012) 15030–15035, <https://doi.org/10.1073/pnas.1205943109>.
- [45] Y. Xia, Z.Y. Yang, P. Xia, T. Hackl, E. Hamel, A. Mauger, J.H. Wu, K.H. Lee, Antitumor agents. 211. Fluorinated 2-phenyl-4-quinolone derivatives as antimitotic antitumor agents, *J. Med. Chem.* 44 (2001) 3932–3936, <https://doi.org/10.1021/jm0101085>.
- [46] Z. Li, C. Mu, B. Wang, J. Jin, Graveoline analogs exhibiting selective acetylcholinesterase inhibitory activity as potential lead compounds for the treatment of Alzheimer's disease, *Molecules* 21 (2016), <https://doi.org/10.3390/molecules21020132>.
- [47] Y. Xie, J. Zhong, Y. Li, X. Xiao, L. Zou, Y. Liu, K. Zhang, J. He, Iodination and O-arylation of 2-arylquinolin-4(1H)-one with Ph(OAc)₂ under metal-free conditions, *Chemistry* 3 (2018) 1655–1657, <https://doi.org/10.1002/slct.201800197>.
- [48] M.S.A. Elsayed, Y. Su, P. Wang, T. Sethi, K. Agama, A. Ravji, C.E. Redon, E. Kiselev, K.A. Horzmann, J.L. Freeman, Y. Pommier, M. Cushman, Design and synthesis of chlorinated and fluorinated 7-azaindenoisoquinolines as potent cytotoxic anticancer agents that inhibit topoisomerase I, *J. Med. Chem.* 60 (2017) 5364–5376, <https://doi.org/10.1021/acs.jmedchem.6b01870>.
- [49] S.R. Laplante, F. Bilodeau, N. Aubry, J.R. Gillard, J. O'Meara, R. Coulombe, N-versus O-alkylation: utilizing NMR methods to establish reliable primary structure determinations for drug discovery, *Bioorg. Med. Chem. Lett* 23 (2013) 4663–4668, <https://doi.org/10.1016/j.bmcl.2013.06.007>.
- [50] M. Hadjeri, A.M. Mariotte, A. Boumendjel, Alkylation of 2-phenyl-4-quinolones: synthetic and structural studies, *chem, Pharm. Bull.* 49 (2001) 1352–1355, <https://doi.org/10.1248/cpb.49.1352>.
- [51] M.S. Schmidt, P. Arroyo Mañez, C.A. Stortz, I.A. Perillo, D. Vega, M.M. Blanco, Alkylation of 2- and 3-alkoxycarbonyl-4-quinolinones. DFT study on the regioselectivity, *J. Mol. Struct.* 1128 (2017) 142–150, <https://doi.org/10.1016/j.molstruc.2016.08.057>.
- [52] R.H. Shoemaker, The NCI60 human tumour cell line anticancer drug screen, *Nat. Rev. Canc.* 6 (2006) 813–823, <https://doi.org/10.1038/nrc1951>.
- [53] M.R. Boyd, K.D. Paull, Some practical considerations and applications of the national cancer institute in vitro anticancer drug discovery screen, *Drug Dev. Res.* 34 (1995) 91–109, <https://doi.org/10.1002/ddr.430340203>.
- [54] P. Skehan, R. Storeng, D. Scudiero, A. Monks, J. McMahon, D. Vistica, J.T. Warren, H. Bokesch, S. Kenney, M.R. Boyd, New colorimetric cytotoxicity assay for anticancer-drug screening, *J. Natl. Cancer Inst.* 82 (1990) 1107–1112, <https://doi.org/10.1093/jnci/82.13.1107>.
- [55] T.S. Dexheimer, Y. Pommier, DNA cleavage assay for the identification of topoisomerase I inhibitors, *Nat. Protoc.* 3 (2008) 1736–1750, <https://doi.org/10.1038/nprot.2008.174>.
- [56] S. Antony, M. Jayaraman, G. Laco, G. Kohlhaagen, K.W. Kohn, M. Cushman, Y. Pommier, Differential induction of topoisomerase I-DNA cleavage complexes by the indenoisoquinoline MJ-III-65 (NSC 706744) and camptothecin: base sequence analysis and activity against camptothecin-resistant topoisomerases I, *Canc. Res.* 63 (2003) 7428–7435.
- [57] SwissADME, n.d. <http://www.swissadme.ch/index.php>.
- [58] A. Daina, O. Michielin, V. Zoete, SwissADME: a free web tool to evaluate pharmacokinetics, drug-likeness and medicinal chemistry friendliness of small molecules, *Sci. Rep.* 7 (2017) 1–13, <https://doi.org/10.1038/srep42717>.
- [59] A. Daina, O. Michielin, V. Zoete, ILOGP: a simple, robust, and efficient description of n-octanol/water partition coefficient for drug design using the GB/SA approach, *J. Chem. Inf. Model.* 54 (2014) 3284–3301, <https://doi.org/10.1021/ci500467k>.
- [60] W.M. Eldehna, A.M. El Kerdawy, G.H. Al-Ansary, S.T. Al-Rashood, M.M. Ali, A.E. Mahmoud, Type IIA - type IIB protein tyrosine kinase inhibitors hybridization as an efficient approach for potent multikinase inhibitor development: design, synthesis, anti-proliferative activity, multikinase inhibitory activity and molecular modeling of novel ind, *Eur. J. Med. Chem.* 163 (2019) 37–53, <https://doi.org/10.1016/j.ejmech.2018.11.061>.
- [61] C.A. Lipinski, F. Lombardo, B.W. Dominy, P.J. Feeney, Experimental and computational approaches to estimate solubility and permeability in drug discovery and development settings, *Adv. Drug Deliv. Rev.* 64 (2012) 4–17, <https://doi.org/10.1016/j.addr.2012.09.019>.
- [62] A.V. Butin, S.K. Smirnov, T.A. Stroganova, W. Bender, G.D. Krapivin, Simple route to 3-(2-indolyl)-1-propanones via a furan recyclization reaction, *Tetrahedron* 63 (2007) 474–491, <https://doi.org/10.1016/j.tet.2006.10.056>.
- [63] S. Zhao, Y. hong He, D. Wu, Z. Guan, A new general approach to 4-substituted-3-halo-2-quinolones, *J. Fluor. Chem.* 131 (2010) 597–605, <https://doi.org/10.1016/j.jfluchem.2010.01.008>.
- [64] M.F. Abo-Ashour, W.M. Eldehna, R.F. George, M.M. Abdel-Aziz, M.M. Elaasser, N.M. Abdel Gawad, A. Gupta, S. Bhakta, S.M. Abou-Seri, Novel indolethiazolidinone conjugates: design, synthesis and whole-cell phenotypic evaluation as a novel class of antimicrobial agents, *Eur. J. Med. Chem.* 160 (2018) 49–60, <https://doi.org/10.1016/j.ejmech.2018.10.008>.
- [65] W.M. Eldehna, G.S. Hassan, S.T. Al-Rashood, T. Al-Warhi, A.E. Altyar, H.M. Alkahtani, A.A. Almehezia, H.A. Abdel-Aziz, Synthesis and in vitro anticancer activity of certain novel 1-(2-methyl-6-arylpyridin-3-yl)-3-phenylureas as apoptosis-inducing agents, *J. Enzym. Inhib. Med. Chem.* 34 (2019) 322–332, <https://doi.org/10.1080/14756366.2018.1547286>.